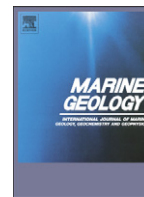




Contents lists available at ScienceDirect

Marine Geology

journal homepage: [www.elsevier.com/locate/margeo](http://www.elsevier.com/locate/margeo)

## The 2.6 Ma depositional sequence from the Challenger cold-water coral carbonate mound (IODP Exp. 307): Sediment contributors and hydrodynamic palaeo-environments

M. Thierens<sup>a,\*</sup>, J. Titschack<sup>b</sup>, B. Dorschel<sup>a</sup>, V.A.I. Huvenne<sup>c</sup>, A.J. Wheeler<sup>a</sup>, J.-B. Stuu<sup>d,e</sup>, R. O'Donnell<sup>a</sup>

<sup>a</sup> *Geology Department and Environmental Research Institute, University College Cork, Lee Road, Cork, Ireland*

<sup>b</sup> *GeoZentrum Nordbayern, Fachgruppe Paläoumwelt, Friedrich-Alexander-Universität Erlangen-Nürnberg, Loewenichstr. 28, 91054 Erlangen, Germany*

<sup>c</sup> *Geology & Geophysics, National Oceanography Centre, Southampton, European Way, Southampton, SO14 3ZH, UK*

<sup>d</sup> *MARUM, Center for Marine Environmental Sciences, University of Bremen, P.O. Box 330440, D-28334 Bremen, Germany*

<sup>e</sup> *Royal Netherlands Institute for Sea Research, P.O. Box 59, NL-1790 AB Den Burg, the Netherlands*

### ARTICLE INFO

#### Article history:

Received 5 August 2009

Received in revised form 19 February 2010

Accepted 23 February 2010

Available online 2 March 2010

Communicated by D.J.W. Piper

#### Keywords:

cold-water coral carbonate mound  
NE Atlantic  
sediment dynamics  
siliciclastic grain-size  
end-member modelling  
grain-surface microtextures

### ABSTRACT

During IODP Expedition 307, the first complete sequence through a cold-water coral carbonate mound (a bio-geological seafloor feature created through successive stages of cold-water coral mediated sediment accumulation) was successfully acquired. The full recovery of the Challenger Mound, one of the large (ca. 155 m high) coral carbonate mounds along the NE Atlantic continental margin (Belgica mound province, eastern Porcupine Seabight) facilitates for the first time the study of the entire development of a coral carbonate mound and, hence, allows the identification of the environmental conditions driving and maintaining the entire build-up of these remarkable seafloor habitats.

In this study, the different sediment contributors to the Challenger Mound are identified and assessed throughout its entire 2.6 Ma long development. High-resolution siliciclastic particle-size end-member modelling and its ground-truthing (XRD, quartz-sand surface microtextures) indicate the influence of an all dominant contour-current system, operating in variable energetic modes, for most of the sediment accumulation history of the Challenger Mound. Only local, short-distance current-controlled sediment re-dispersal is evidenced, while iceberg rafting is identified as an important depositional mechanism throughout the whole mound development period. Furthermore, evidence for icebergs repeatedly reaching the eastern Porcupine Seabight continental margin, even in the early stages of Northern Hemisphere glacial expansion, is preserved in the mound sequence.

Supporting the existing coral-stratigraphy, the Challenger Mound depositional sequence reveals a two-phase development, separated by a significant hiatus. The lower mound-phase (M1; 2.6–1.7 Ma) indicates a semi-continuous, steadily changing, fast accumulating current-controlled depositional environment. The condensed upper mound-phase (M2; 998–1.5 ka) bears witness of a distinct shift to a more glacially-influenced, low accumulation environment, most likely resulting from a reduced capacity to deposit and/or preserve sediments. Cold-water coral density at the site of deposition is assumed to play an essential role in sediment deposition and preservation on Challenger Mound. It enabled the preservation of a unique, higher resolution record in the lower M1 sequence in the otherwise erosive/non-depositional Early-Pleistocene environment along the NW European continental margin. The potential of coral carbonate mounds as intermediate water depth, continental margin, (Plio-)Pleistocene palaeo-archives is thereby showcased.

© 2010 Elsevier B.V. All rights reserved.

### 1. Introduction

In specific marine settings, framework-building cold-water corals (azooxanthellate scleractinians such as *Lophelia pertusa* and *Madrepora oculata*) are the founders of intriguing seafloor habitats, the so-called coral carbonate mounds (sensu Roberts et al., 2009). Especially

along the Irish Atlantic continental margin (see Roberts et al., 2006; Wheeler et al., 2007 and references therein), cold-water corals successfully mediated sediment accumulation, creating a variety of coral carbonate mound structures, from small (semi-)buried features to “giant” mounds with heights up to several hundred metres (Wheeler et al., 2007 and references therein).

The successful development of these bio-geological built-ups seems to rely predominantly on the co-occurrence of the optimal environmental conditions (mainly water temperature, current strength, sediment and food availability) for both coral growth and

\* Corresponding author. Tel.: +353 21 490 1947; fax: +353 21 490 1932.  
E-mail address: [mieke.thierens@gmail.com](mailto:mieke.thierens@gmail.com) (M. Thierens).

sediment accumulation, as shown from studies of (sub-)recent coral carbonate mound material (e.g. Freiwald, 2002; Dorschel et al., 2007; Mienis et al., 2007; Wheeler et al., 2007; White et al., 2007). The presence of these optimal conditions is linked to the temperature–salinity gradients at water-mass boundaries (Rüggeberg et al., 2007; White, 2007; White et al., 2007; Dullo et al., 2008), whose positions in the Porcupine Seabight appeared especially favourable during the intermediate climatic stages of the Late Pleistocene–Holocene (Dorschel et al., 2005; Rüggeberg et al., 2007).

Without the presence of a full mound sequence (sensu Henriet et al., 2002: documenting mound initiation till decline), however, uncertainty remained about the role of these environmental processes in mound initiation and their relevance throughout the entire mound development period. Therefore, Challenger Mound, one of the large (ca. 155 m high) coral carbonate mounds along the NE Atlantic continental margin (Belgica mound province, eastern Porcupine Seabight; Fig. 1), was targeted during the IODP Expedition 307 drilling (Ferdelman et al., 2006; Williams et al., 2006). The complete recovery of this coral carbonate mound sequence allows, for the first time, the study of an entire mound's development and its drivers.

As sedimentary input and prevailing hydrodynamic regime directly influence the availability of food and sediment particles in and to the coral carbonate mound system (Duineveld et al., 2007; Mienis et al., 2007; White, 2007), they represent key controls on recent coral carbonate mound development. To assess their importance through time, this study attempts to reconstruct the hydrodynamic environment and its variability throughout the (Plio-) Pleistocene development of the Challenger Mound. High-resolution siliciclastic particle-size data are processed and ground-truthed, by means of end-member modelling (cf. Weltje, 1997), XRD phase quantification and quartz-sand surface microtextures, to identify and characterise the different sediment contributors that influenced the Challenger Mound system.

## 2. General setting

### 2.1. Porcupine Seabight

Southwest of Ireland, the Porcupine Seabight forms a shallow to deep-water, north–south trending embayment in the north-east Atlantic continental margin, only connected to the deeper North Atlantic (Porcupine Abyssal Plain) via a narrow passage in the southwest (Fig. 1A). The Porcupine Basin is one of the failed-rift sedimentary basins created during the opening of the North Atlantic Ocean (Shannon et al., 2007). Cenozoic post-rift sediment accumulation was affected by several regional erosion events, related to NE Atlantic tectonic and oceanographic reorganisations (Stoker et al., 2005). The youngest of these unconformities (RD1; see Section 2.2) appears to serve as initiation point of coral carbonate mound growth in the Porcupine Seabight (De Mol et al., 2002).

Three well-defined clusters of coral carbonate mounds (provinces) are described in the Porcupine Seabight, with the Magellan and Hovland mound provinces situated in the north of the Seabight (450–900 m water depth) (De Mol et al., 2002) and the Belgica Mounds on the eastern flank, between 550 and 1025 m water depth (De Mol et al., 2007) (Fig. 1A).

In the present-day hydrographic setting, the water masses in the depth range of the mounds consist of Eastern North Atlantic Water (ENAW; upper 800 m) overlying the Mediterranean Outflow Water (MOW; 800–1100 m) (Rice et al., 1991; New et al., 2001; White, 2007). Both water masses are carried northwards along the continental margin: the ENAW as part of the upper-slope Shelf Edge Current and the MOW as an intermediate contour-current flowing from the Gulf of Cadiz along the Portuguese and Irish margins, cyclonically along Porcupine Seabight, as far as the Porcupine Bank/Rockall Trough area (Pingree and Le Cann, 1989; Rice et al., 1991; New et al., 2001).

Along the eastern Porcupine Seabight margin a persistent, north-westward directed residual current, varying between 5 and 15 cm s<sup>-1</sup>, has been recorded by Dorschel et al. (2007) and White et al. (2007) in the Belgica mound province (BMP). Current speeds in this region are generally high (mean: 16–25 cm s<sup>-1</sup>), at peak events even exceeding 60 cm s<sup>-1</sup>, as the result of topographically steered bottom-current enhancement (Dorschel et al., 2007; White, 2007; White et al., 2007). White (2007) and White et al. (2007) illustrated that the rectification of baroclinic, diurnal period tidal currents on the eastern slope causes enhanced tidal motions across-slope and a stronger daily residual flow along-slope. As White (2007) indicated, all conditions for maximum current intensification on the eastern slope are met at the depth of the permanent pycnocline (being the boundary between ENAW and MOW) between 600 and 800 m water depth, which is well within the water depth range of the BMP mounds.

Evidence of this dynamic benthic environment and the bottom-current-controlled sedimentation in Porcupine Seabight is manifold. For example, seismic imaging and remote sensing surveys have identified sand ripples, sediment waves, erosional moats, significant contourite drift successions and multiple regional unconformities along the eastern margin (e.g. De Mol et al., 2002; Huvenne et al., 2002; Van Rooij et al., 2003; Wheeler et al., 2005, 2007; De Mol et al., 2007). In addition, sediment core studies of Late Pleistocene–Holocene off-mound BMP sediments associate coarser-grained sediments with more vigorous bottom-current regimes during interglacial periods, while reduced current activity and finer-grained sediments are implied for glacial environments (Foubert et al., 2007; Van Rooij et al., 2007). Similar patterns of along-slope current-controlled sedimentation have been uncovered at several locations along the north-east Atlantic continental margin (e.g. Hall and McCave, 2000; Weaver et al., 2000; Laberg et al., 2005; Øvrebo et al., 2006). Furthermore, magnified across-slope directed tidal currents induce resuspension of slope sediments and, hence, enable the formation of bottom and intermediate nepheloid layers, as described in the area by, e.g., Rice et al. (1991) (Porcupine Seabight), Dickson and McCave (1986) (Porcupine Bank), Mienis et al. (2007) (S Rockall Trough) and McCave et al. (2001) (Goban Spur).

In contrast to elsewhere on the continental margin (e.g. Weaver et al., 2000) no major reports of turbidite or other down-slope mass-transport deposits have been made thus far for the eastern Porcupine Seabight. Van Rooij et al. (2003) described potential, minor and local turbiditic channels flanking mounds in the BMP, although their formation by bottom-currents cannot fully be excluded. In addition, the only down-slope channel system in the Seabight is located on its southern margin (Gollum Channel System), where it is currently considered inactive in terms of mass sediment transport (Kenyon et al., 1978; Wheeler et al., 2003). A limited contribution of down-slope sedimentation processes is therefore implied at present. On the other hand, substantial evidence of Late Pleistocene glacial iceberg rafting is found in and around Porcupine Seabight (Belderson et al., 1973; Games, 2001; Øvrebo et al., 2006; Dorschel et al., 2007; Foubert et al., 2007; Peck et al., 2007; Van Rooij et al., 2007), nominating ice-rafting as an undeniable sediment input source for the area (cf. Ruddiman, 1977). In the BMP, Van Rooij et al. (2007) were able to associate these ice-rafted deposits with the evolution of the proximal British–Irish Ice Sheet (BIIS).

### 2.2. The Challenger coral carbonate mound

The Challenger Mound is one of the large (ca. 155 m high; Ferdelman et al., 2006) coral carbonate mounds situated on the eastern Porcupine Seabight continental margin (Fig. 1). It is included in the Belgica mound province (BMP; Fig. 1A–B), as one of the 47 exposed mounds documented in this part of the continental slope (550–1025 m water depth; De Mol et al., 2007).

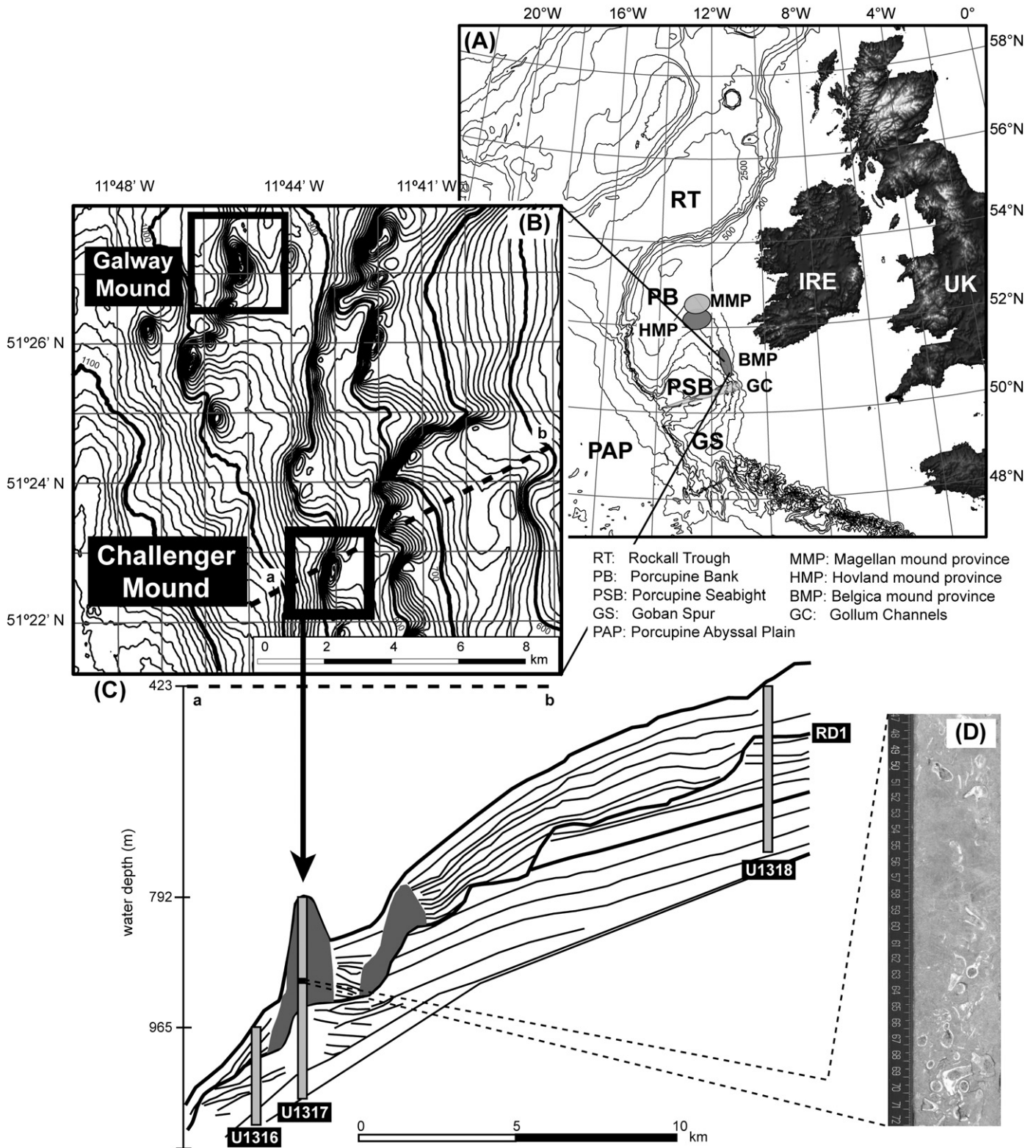


**Fig. 1.** Location of Challenger Mound on the eastern Porcupine Seabight (PSB) continental margin. (A.) Overview map of PSB, with the Belgica mound province (BMP) located on its eastern flank. Bathymetry (500 m contour interval) based on [GEBCO \(2003\)](#). (B.) Bathymetric expression (10 m contour interval) of the Challenger Mound and neighbouring Galway Mound within the BMP (based on [Beyer et al., 2003](#)). Transect a–b orientating the profile described in (C.). (C.) Interpreted seismic profile (adapted from [De Mol et al., 2002](#)) across the IODP Exp. 307 transect, indicating the position of the Challenger Mound (U1317), its adjacent off-mound drill sites (U1316, U1318) and the regional unconformity RD1 ([Van Rooij et al., 2003](#)) which is found at the base of Challenger Mound. Water depths of the drill sites for reference ([Ferdelman et al., 2006](#)). (D.) Challenger Mound core surface photograph illustrating the typical embedding of framework-building cold-water corals in a sedimentary matrix of mixed siliciclastic/pelagic carbonate origin.

The Challenger Mound, as all Porcupine Seabight coral carbonate mounds ([De Mol et al., 2002](#)), is rooted on the RD1 unconformity ([Van Rooij et al., 2003](#)) (Fig. 1C). This regional, multi-phase, Late Miocene–

Late Pliocene erosion event is attributed to the major oceanographic changes at the onset of Northern Hemisphere glaciation ([Stoker et al., 2005](#); [Van Rooij et al., 2009](#)), and the (re-)introduction of MOW in the

Porcupine Seabight in particular (De Mol et al., 2002; Van Rooij et al., 2003). It created a sharp firmground at the base of the mound, separating the underlying, Miocene glauconitic siltstones from the (Plio-)Pleistocene mound sequence (Ferdelman et al., 2006; Williams et al., 2006; Kano et al., 2007). The IODP Exp. 307 Challenger Mound drilling evidenced, for the first time, the presence of cold-water coral fragments (mainly *Lophelia pertusa*) throughout the entire mound sequence (Ferdelman et al., 2006; Williams et al., 2006). Varying quantities of these coral fragments are found embedded in an un lithified, mixed siliciclastic/pelagic-carbonate matrix (Fig. 1D; Titschack et al., 2009). Coral growth started around 2.7 Ma (Kano et al., 2007), after which sediments began to accumulate between the coral branches (ca. 2.6 Ma; Foubert and Henriët, 2009), hence initiating the formation of the mound structure. The *Lophelia pertusa*  $^{87}\text{Sr}/^{86}\text{Sr}$  stratigraphic record reveals a major hiatus in the sequence, from 1.7 to 1 Ma (ca. 23 m depth; Kano et al., 2007), demarcating two main phases of coral growth in the Challenger Mound. At present, only dead coral rubble is found covering the mound. IODP Exp. 307 site U1318 investigations (Huvenne et al., 2009b; O'Donnell, pers. comm.) indicate the restart of off-mound drift accumulation (mainly silty contourites) since ca. 1.24 Ma, which has since then partially buried the upslope flank of Challenger Mound (Fig. 1C).

### 3. Materials and methods

This study focuses on the Challenger Mound sediments recovered during the IODP Exp. 307 hole U1317E drilling (51°22.8'N, 11°43.1'W; 792.2 m water depth). Advanced piston coring allowed penetration to a depth of 158.6 metre below seafloor (mbsf; all depths are corrected for decompaction), acquiring a complete mound sequence (0–155.22 mbsf) from the summit of this coral carbonate mound structure (Ferdelman et al., 2006).

#### 3.1. Age model

As part of this study, the top sediment of U1317E was dated by  $^{14}\text{C}$  accelerator mass spectrometer (AMS) dating on planktonic foraminifera (multi-species >150  $\mu\text{m}$ ) at the Beta Analytic Radiocarbon Dating Laboratory, Inc. The data is  $\delta^{13}\text{C}$ -corrected and calibrated using the INTCAL04 database (Reimer et al., 2004) with corrections for the marine reservoir effect.

The *Lophelia pertusa*  $^{87}\text{Sr}/^{86}\text{Sr}$  age model by Kano et al. (2007) provides a stratigraphic framework for the cold-water coral evolution in Challenger Mound. For stratigraphic reference of sediment accumulation, this study combines the  $^{14}\text{C}$  AMS date with the

event-based, sediment magnetostratigraphy by Foubert and Henriët (2009) (Fig. 3). This is preferred over the more continuous oxygen-isotope stratigraphy by Sakai et al. (2009), as Titschack et al. (2009) identified several potential unconformities throughout the sedimentary sequence.

#### 3.2. Siliciclastic particle-size analysis

For this study, the U1317E mound cores were sub-sampled at a 10 cm resolution, generating a total of 1504 ca. 1 cm<sup>3</sup> samples for particle-size analysis (PSA). Both organic matter and the carbonate phase were removed through oxidation (10% H<sub>2</sub>O<sub>2</sub>) and dissolution (10% HCl), respectively, in order to obtain the siliciclastic matrix fraction, which is considered to contain all relevant hydrodynamic information (McCave et al., 1995). Biogenic silica was not removed as it appeared to be negligible. Prior to measurement all sediments were fully disaggregated and dispersed by adding a 0.05% Calgon (Sodium Hexametaphosphate) solution and continuous shaking for at least 12 h. The particle-size distributions of the siliciclastic fraction were measured on a Malvern Mastersizer 2000 laser-granulometer (size-range: 0.02 to 2000  $\mu\text{m}$ ) with Autosampler and Hydro G dispersion unit at the National Oceanography Centre Southampton (measurement settings in Table 1). For every sample the distributions of three consecutive PSA runs were checked for consistency and the appropriate distributions were averaged to create the final size distribution. An assessment of the sample representativeness and the measurement precision of the instrument, based on 235 replicate and 58 repetitive measurements, indicates an average PSA mode error of 4.41% (Table 1).

Standard statistical parameters (modal size, sorting and kurtosis) of the PSA distributions were calculated according to Folk and Ward (1957) as implemented in the GRADISTAT software (Blott and Pye, 2001). As not only bottom-currents are likely to affect the U1317E study site (Section 2.1), the sortable-silt approach by McCave et al. (1995) is not considered applicable in this study.

#### 3.3. Particle-size end-member modelling

To meaningfully identify the different sedimentary processes affecting the siliciclastic accumulation of Challenger Mound, the end-member modelling algorithm (EMMA) by Weltje (1997) is applied to the particle-size dataset. As demonstrated in several studies and a range of marine environments (e.g. Prins and Weltje, 1999; Prins et al., 2002; Stuut et al., 2002; Frenz et al., 2003; Weltje and Prins, 2003; Stuut et al., 2007) this algorithm proves most

**Table 1**

Malvern measurement settings (A.) and assessment of sample representativeness (B.) and instrument measurement precision (C.) for U1317E samples and the Malvern Mastersizer 2000 laser-granulometer at the National Oceanography Centre Southampton (UK).  $N$  = number of samples in (sub-) dataset;  $n_1$  = total number of replicate measurements (2–3 per sample);  $n_2$  = total number of repetitive measurements (2–5 per sample).

(A.) Malvern settings	(B.) Replicate measurements					(C.) Repetitive measurements				
	Sediment type	N	Mode range ( $\mu\text{m}$ )	Mode error (%) <sup>a</sup>	$R^{2b}$	N	Mode range ( $\mu\text{m}$ )	Mode error (%) <sup>a</sup>	$R^{2b}$	
Material properties										
Refraction index	1.52									
Absorption	0.01									
Pump speed rpm	2300	All types	114	6–128	4.41	0.99	21	6–218	3.63	0.99
Obscuration	15%		[ $n_1=235$ ]				[ $n_2=58$ ]			
Ultrasonification	10 s	Fine	15	<10	6.68	0.97	2	<10	0.88	0.99
Measurement time		Intermediate	30	10–50	6.51	0.99	8	10–50	5.25	0.99
Sample	25 s	Coarse	37	>50	3.47	0.99	5	>50	3.42	0.99
Background	25 s	Bimodal	32	6–100	3.02	0.98	6	6–208	2.58	0.98

<sup>a</sup>Average mode error for all samples in sub-dataset [per sample calculated as: (1 SD/average mode) × 100].

<sup>b</sup>Average correlation between replicate/repetitive and original measurements for all samples in sub-dataset.

powerful in deconvoluting grain-size distributions into physically meaningful and dataset-specific sub-populations, the so-called end-members. Each of these end-member size distributions is assumed to represent an elementary sub-assemblage of grains that originated from statistically indistinguishable provenance and/or transport processes (Prins and Weltje, 1999; Weltje and Prins, 2003). In this way, EMMA enables identification of the different sediment contributors affecting the sedimentary system under investigation and permits further meaningful interpretations.

End-member modelling involves a two-step process in which, first of all, the appropriate amount of end-members is chosen as the compromise of the best fit (indicated by the coefficient of determination  $r^2$ ) with the least amount of end-members. Afterwards the relative contribution of each end-member can be calculated for every individual particle-size distribution.

Goodness-of-fit statistics for the Challenger Mound end-member model (Fig. 2A–B) indicate the adequacy of a four end-member model. With four end-members 83% of the variance in the particle-size dataset is explained by the model ( $r^2 = 0.83$ ), which is comparable to previous studies (e.g. Prins et al., 2002:  $r^2 = 0.84$ ; Frenz et al., 2003:  $r^2 = 0.87$ ). With an increasing number of end-members a better fit can be obtained (e.g. 5 end-members: mean  $r^2 = 0.85$ ), particularly in the finer size ranges ( $<10\ \mu\text{m}$ ). However, this improvement is not regarded as significant enough to justify an additional end-member, as the risk of modelling noise instead of signal becomes more likely. An example of the EMMA unmixing of a Challenger Mound sample is given in Fig. 2C.

Ground-truthing end-members, i.e. interpreting them in terms of actual provenance, transport and post-depositional processes by means of additional, independent analyses, is a last vital step in the end-member modelling procedure. In this study, XRD mineral quantification of the siliciclastic sediment fraction and quartz grain-surface microtextural analysis are chosen as providers of both provenance and transport information.

### 3.4. XRD phase quantification

A total of 57 representative samples, capturing varying abundances of all four end-members in a range of combinations, were selected from the end-member dataset for further ground-truthing. Circa 3 g of bulk matrix sediment was prepared for mineral quantification by X-ray diffraction (XRD) according to the standardised procedures of the mineralogical lab at the GeoZentrum Nordbayern (see Titschack et al., 2009). At this facility, XRD profiles were acquired with a Siemens D5000 diffractometer (Bragg–Brentano geometry) for an angular range of  $5\text{--}70^\circ$  at a step size of  $0.02^\circ$  and 2 s counting time per step.

Interpretation and semi-quantification of mineral phases (1 weight% [wt.%] detection limit) was accomplished by means of the Rietveld refinement software TOPAS 3.0 with fundamental parameter approach (Cheary and Coelho, 1992; Cheary et al., 2004; Titschack et al., 2009 for methodological remarks).

Phase abundances (wt.%) within the siliciclastic matrix fraction were computed after removal of the carbonate (calcite, dolomite and aragonite) and authigenic phases (gypsum and halite) from the bulk XRD quantifications.

### 3.5. Quartz grain-surface microtextures

Quartz grains from 16 samples, dominated by the coarser-grained end-members EMc and EMd (see Section 4), were investigated in detail for grain-surface microtextural evidence of their origin. Very fine to medium sand-sized quartz grains ( $63\text{--}360\ \mu\text{m}$ , cf. Helland and Holmes, 1997; Mahaney and Kalm, 2000) were targeted in this study to capture a significant fraction of grains that should allow the identification of the coarse siliciclastic input, while minimizing the

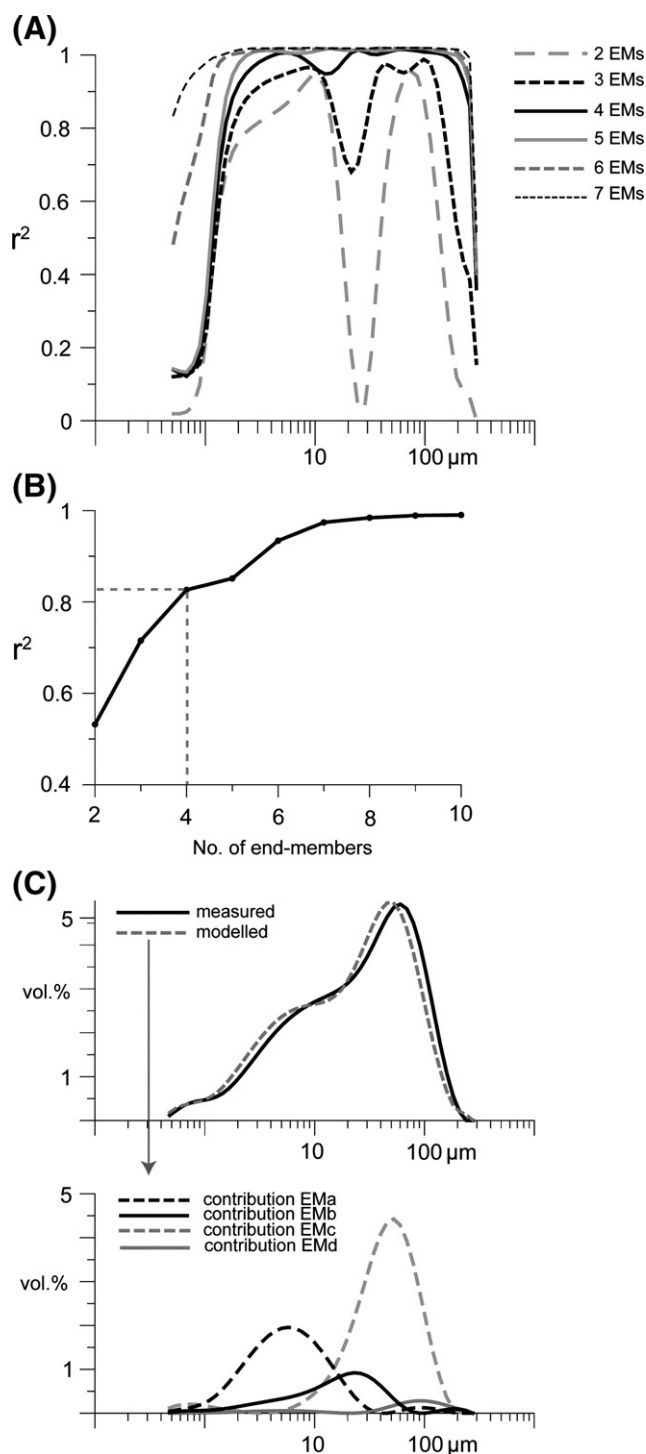


**Fig. 2.** End-member modelling of Challenger Mound (U1317E) particle-size data. (A.) Goodness-of-fit statistic ( $r^2$ ) per size class for U1317E end-member models with 2–7 end-members. (B.) Overall mean goodness-of-fit ( $r^2$ ) for U1317E end-member models with 2–10 end-members. With 4 end-members a fit of  $r^2 = 0.83$  is obtained. (C.) Application of the 4 end-member model to an U1317E particle-size sample. The offset between measured and modelled particle-size distributions (volume %) (above) is illustrated, as well as the individual contributions of the four end-members (EMa–b–c–d) to the total fit (below).

effect of varying grain-size and lithology on surface texture variation (Ingersoll, 1974; Dowdeswell, 1982).

Circa  $0.3\ \text{cm}^3$  of bulk sediment was disaggregated by ultrasonification (30 s) and subsequently filtered ( $5\ \mu\text{m}$  mesh size) to remove heavy surface coatings by adhering fine particles. Dried samples were mounted on aluminium stubs and sputter coated with gold (Polaron

E5150 Sputter Coating Unit) in preparation for scanning electron microscopic analysis at the Electron Microscopy Facility, University College Cork.

From each sample (7 EMc- and 9 EMD-dominated samples) 11–19 sand-sized quartz grains were selected at random, with each grain verified as quartz using an INCA x-sight Energy Dispersive X-ray Spectroscopy Detector (Oxford Instruments) in secondary electron mode (acceleration voltage of 20 kV at 20 mm working distance; 0–20 keV spectra obtained for a 100 s live-time period). Subsequently, the surfaces of all 246 grains under study were imaged with a JEOL JSM 5510 Scanning Electron Microscope (acceleration voltage of 5 kV at 10 mm working distance) and the presence, absence and frequency of occurrence (cf. Cater, 1987) of 23 diagnostic surface features (see Table 2) was evaluated and recorded. A combination of feature occurrence and dominance data are used to identify different grain types and their abundance within the samples and to compare them to those reported from a series of glacial and non-glacial sedimentary environments (e.g. Ingersoll, 1974; Manker and Ponder, 1978; Higgs, 1979; Hill and Nadeau, 1984; Dowdeswell et al., 1985; Helland and Holmes, 1997; Mahaney and Kalm, 2000; Mahaney, 2002; Strand et al., 2003; Damiani et al., 2006; St. John, 2008).

## 4. Results

### 4.1. Siliciclastic particle-size analysis

Overall the siliciclastic particle-size distributions of the Challenger Mound matrix can be described as (very) poorly sorted (2.6–5.6 sorting; 3.6 on average), platy- to mesokurtic (0.7–1.6; 0.9 on average) and silt-dominated (Fig. 3). The silt-size-fraction comprises between 28 and 93% (77% on average) of the total siliciclastic sediment volume (vol.%), while the clay-size-range only contributes between 1 and 9 vol.% (6 vol.% mean). Sand-sized grains account, on average, for ca. 17 vol.% of sediment, but a number of clear deviations from this average can be noted downcore, most importantly between 0–1.7 mbsf, 16–27.5 mbsf, 58.8–59.8 mbsf, 67.7–68.1 mbsf and 140.5–146.6 mbsf. These significant peaks in sand particles (up to 50–70 vol.%) correspond to an increased contribution of coarser-grained material (e.g. reflected in the enrichment of the fraction larger than 150  $\mu\text{m}$ ), concurring with an overall deterioration of the sediment sorting (Fig. 3).

Notwithstanding generally broad (low sorting) and medium-peaked (low kurtosis), most Challenger Mound particle-size distributions are unimodal (bimodal curves occur in minor quantities). Two distinct siliciclastic modes can be distinguished in the sequence, a fine silt (ca. 6–10  $\mu\text{m}$ ) and very coarse silt/fine sand (ca. 50–70  $\mu\text{m}$ ) one. Sediments characterised by these two dominant modes are found alternating throughout the mound sequence, especially in the interval

between 27.5 and 155.2 mbsf (Fig. 3). Considerably larger modes (up to 271.3  $\mu\text{m}$ ) and distributions with an intermediate particle-size mode (ca. 30–45  $\mu\text{m}$ ) and slightly better sorting (mean: 3.32), on the other hand, are most frequently identified in the top 27 m of U1317E (Fig. 3).

### 4.2. Particle-size end-member modelling

The four Challenger Mound end-members (EM) all have a clearly different and defined dominant modal size and can be described, from fine to coarser, as follows (Fig. 4A). *EMa* represents a poorly sorted, mesokurtic distribution with a grain-size mode in the fine silt fraction (ca. 6  $\mu\text{m}$ ). *EMb* is equally poorly sorted and mesokurtic in shape, whereas the largest population of grains (dominant mode) can be found around 25  $\mu\text{m}$  (medium silt). The *EMc* distribution is overall better sorted (however, still poorly sorted) and more peaked (leptokurtic) than all other end-member distributions and has a modal size of 56  $\mu\text{m}$ . *EMd*, in contrast to the other end-members, has a clear bimodal particle-size distribution, with a distinct mode in the very fine sand fraction (ca. 98  $\mu\text{m}$ ) and a minor, second mode around 5  $\mu\text{m}$  (fine silt).

No size interval is exclusive to one end-member and no sample can be satisfactorily reproduced by less than two end-members (Fig. 4B). Three out of four end-members (*EMa*–*b*–*c*) are found semi-continuously, each occurring in a minimum of 86% of all samples (minimum abundance of 10%), compared to the more intermittent presence of the fourth end-member (*EMd*; minimum 10% contribution in only 12% of samples). The occurrence of one end-member does not systematically seem to exclude the presence of another one and in 4% of the Challenger Mound samples all four end-members can be distinguished within one sample (Fig. 4B).

Overall *EMc* is the most dominant end-member (dominant in 44% of samples with average proportions of 36%), alternating in dominance with the finer *EMa* (dominant in 33% of samples with an average contribution of 33%). *EMa*, notably, can only be found in dominating proportions in the lower part of U1317E, below ca. 23 mbsf where a significant shift in its abundance values can also be noted (13% average abundance above ca. 23 mbsf compared to 37% below). Conversely, the intermediate *EMb* and coarser *EMd* end-members (overall average abundance of 26% and 4%, respectively) appear more abundant and dominant above ca. 23 mbsf (e.g. mean *EMd* proportions of 15% above ca. 23 mbsf in comparison with only 2% average abundance in the lower depths). In distinct samples end-members reach peak abundances up to 85–87% (*EMa*–*b*–*c*) and 99% (*EMd*) (Fig. 4B).

### 4.3. XRD phase quantification

In all 57 samples six mineral phases are successfully quantified within the siliciclastic fraction (Fig. 5A), which, on average, makes up 63 wt.% of the total matrix sediment. In this non-carbonate phase quartz is found to be the most abundant mineral, varying between 34 and 81 wt.% (mean: 57 wt.%), whereas feldspars (both plagioclase and microcline) only occur in minor quantities (5–17 wt.%; 10 wt.% on average). Three clay minerals have been identified (between 6 and 57 wt.%; 33 wt.% mean), with illite being the most dominant phase (19 wt.% average; 58% of clays) compared to kaolinite (9 wt.% mean; 26% of clays) and chlorite (5 wt.% on average; 16% of clays). This illustrates the variable quantities in which all six siliciclastic phases are identified throughout the U1317E sequence. Downcore, the distinction can be made between samples relatively enriched in quartz (65 wt.% mean; 0–ca. 23 mbsf) and those with a relatively increased clay mineral content (37 wt.% average; ca. 23–155 mbsf).

**Table 2**

List of grain-surface microtextures used in this study. Terminology according to Mahaney (2002), except [13]: overall indication of features produced by mechanical abrasion; [14]: cf. Fig. 6(g) in Damiani et al. (2006); [18]: Higgs (1979).

Outline	Mechanical abrasion features	Chemical abrasion features
1. Low sphericity	8. Conchoidal/linear fractures	18. Solution pits
2. High sphericity	9. Linear/arc-shaped steps	19. Dissolution etching
3. (Sub-)angular	10. Abrasion grooves	20. Mineral precipitation
4. (Sub-)rounded	11. V-shaped percussion cracks	
	12. Craters	
5. High relief	13. Abraded surface	
6. Medium relief	14. Irregular depressions <sup>a</sup>	Overall surface appearance
7. Low relief		
	15. Sharp edges	21. Fresh
	16. Bulbous edges	22. Weathered
	17. Rounded edges <sup>a</sup>	23. Preweathered

<sup>a</sup> Both mechanical and chemical origins are possible.

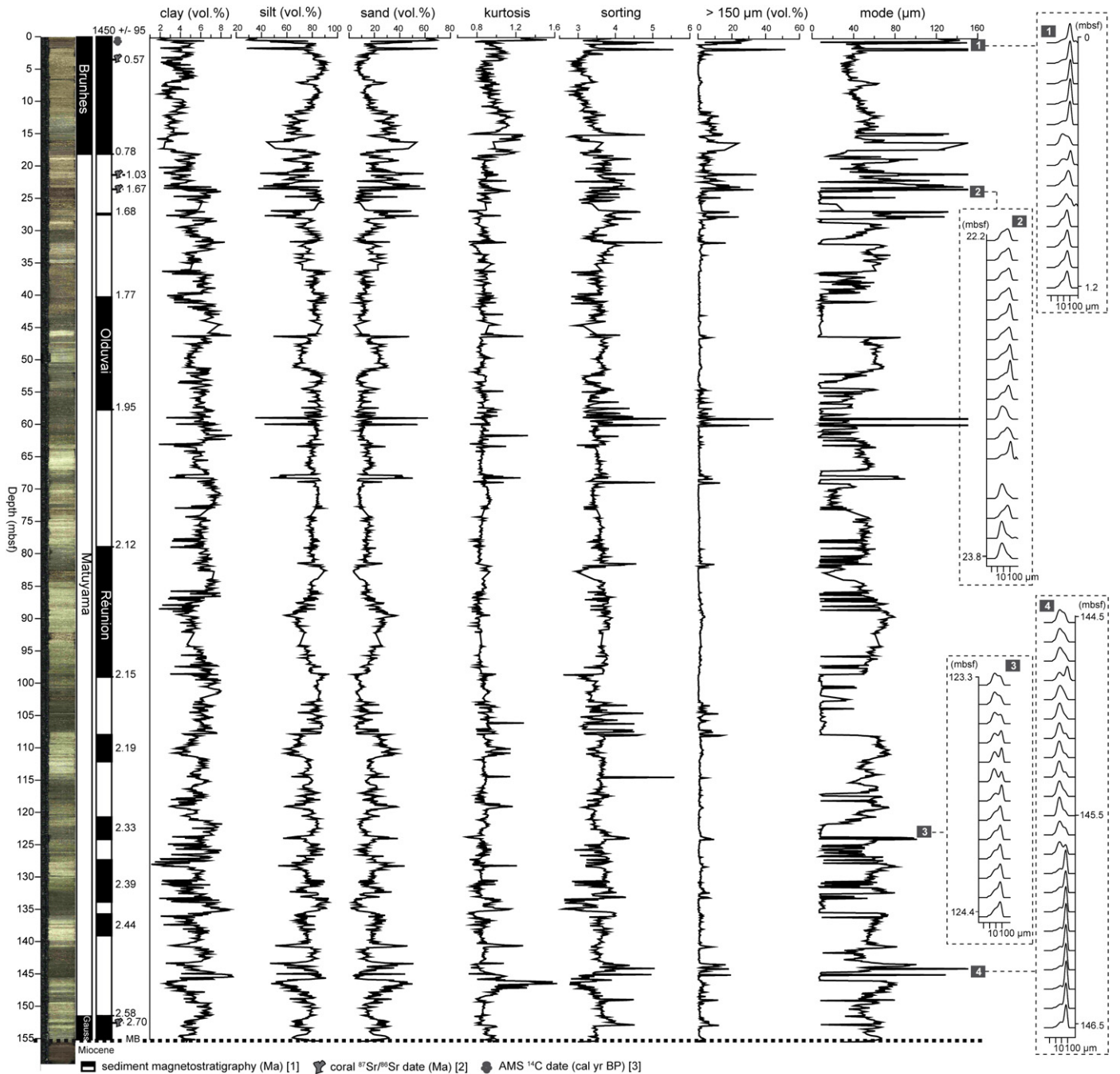


**Fig. 3.** Challenger Mound (U1317E) siliciclastic particle-size results. Downcore variation of particle-size descriptive parameters. Clay (<2 μm), silt (2– 63 μm), sand (>63 μm) and coarser sand (>150 μm) size-fraction contributions in volume % (vol.%). Higher kurtosis and sorting values indicate more peaked and poorer sorted particle-size distributions, respectively. Examples of typical particle-size spectra (0.01–2000 μm; logarithmic scale) from four depth intervals (1–4) throughout the mound sequence are given to the right. All depths in corrected metre below seafloor (mbsf); MB = mound base; [1] Foubert and Henriet (2009), [2] Kano et al. (2007) and [3] this study.

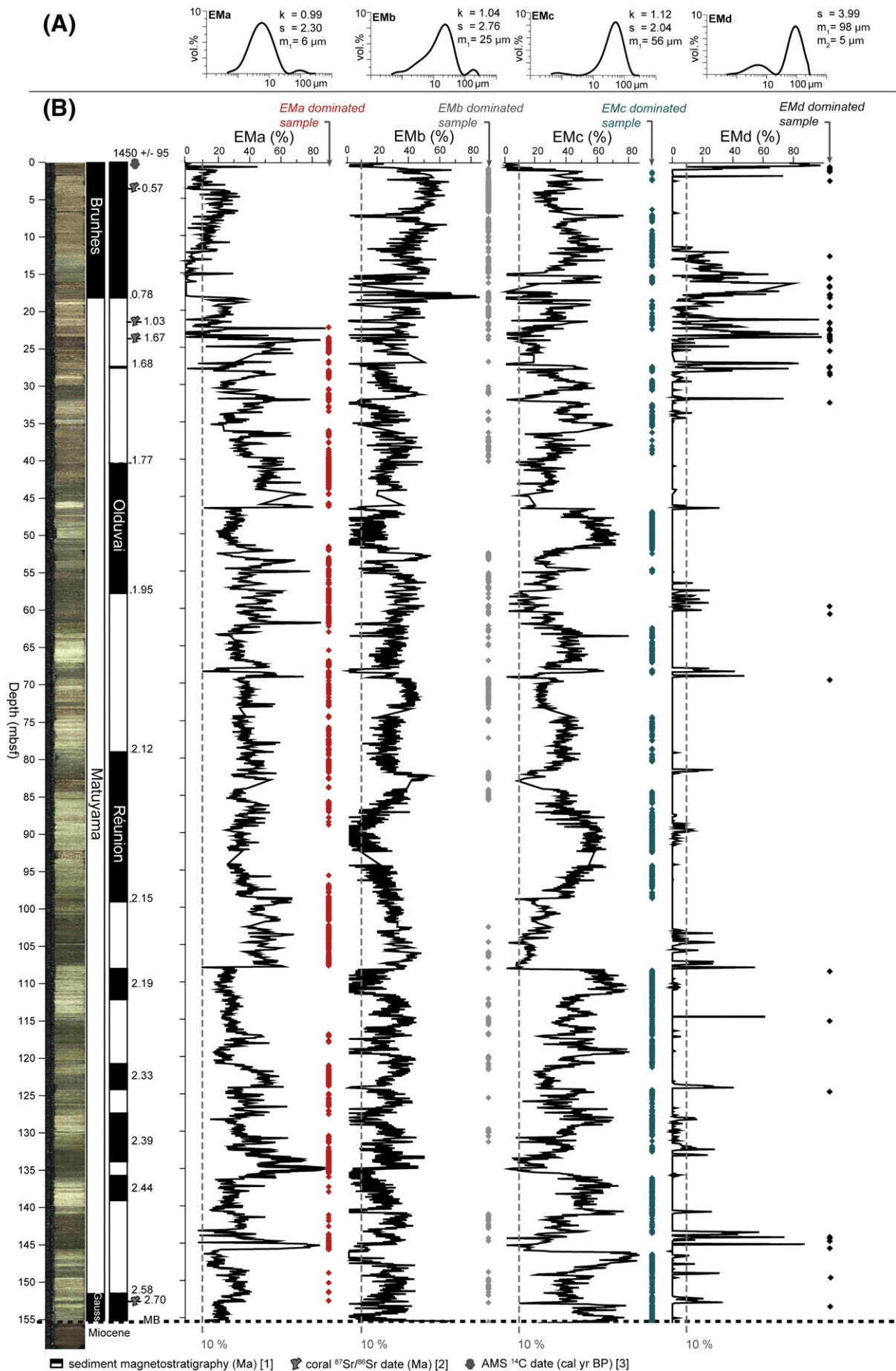
#### 4.4. Quartz grain-surface microtextures

The selected Challenger Mound quartz-sand assemblage consists of mainly sub-angular to sub-rounded grains with a medium relief and low sphericity (Fig. 6). All grains show a broad spectrum of both mechanically and chemically induced grain-surface microtextures

and based on the reoccurring coexistence and, above all, dominance of particular grain-surface features, four distinct grain types are identified (Fig. 6).

*Type 1 grains* (Fig. 6A–B) are (sub-)angular, with sharp edges and a medium to high relief. The grain surfaces are dominated by intense and deeply embedded mechanical abrasion features, such as

**Fig. 4.** Challenger Mound (U1317E) end-member modelling results. (A.) Siliciclastic particle-size distributions (0.01–2000 μm on logarithmic scale; volume %) for the four Challenger Mound end-members (EMA-d), with k = kurtosis, s = sorting, m<sub>1</sub> = primary modal size, m<sub>2</sub> = secondary modal size (bimodal distributions). (B.) Downcore relative abundance (%) of the four end-members (EMA-d; 10% relative contribution as grey dashed line on abundance plots). Dominance of the end-member in a sample is indicated (diamond) downcore next to its abundance plot. All depths in corrected metre below seafloor (mbsf); MB = mound base; [1] Foubert and Henriet (2009), [2] Kano et al. (2007) and [3] this study.



conchoidal fractures, sub-parallel linear fractures, linear and arch-shaped steps and abrasion grooves. V-shaped percussion cracks are observed on more than 50% of these grains, however, rarely covering more than 10% of the grain surface and predominantly as part of a preweathered structure. Similarly, features indicative of chemical alteration (solution pits, mineral precipitation and dissolution etching) mainly occur in minor quantities, illustrating the fresh appearance of most (ca. 60%) Type 1 grain surfaces.

Type 2 grains (Fig. 6C–D) display a similar range of microtextures as Type 1 specimen and also consist of (sub-)angular and medium-relief sands. However, mechanical abrasion features do not dominate the grain surfaces anymore, nor do they reach the intensity of Type 1, while the importance of edge rounding and dissolution etching has increased significantly. Overall, most weathering still appears inherited (preweathered) and about 35% of Type 2 grains possess a chemically unaltered surface.

Type 3 grains (Fig. 6E–F) exhibit predominantly (sub-)rounded outlines with a medium to low relief. Conchoidal fractures, steps, abrasion grooves and V-shaped cracks can be observed in minor quantities although most grain surfaces are heavily overprinted by dissolution features and edge rounding. Reprecipitation of silica and/or other mineral phases is discerned on 38% of these grains, though only a limited surface section is coated by this process. In contrast to the previous grain types, ca. 80% of Type 3 quartz particles are clearly weathered.

Type 4 grains (Fig. 6G–H) are characterised by a very well to sub-rounded outline, medium relief and, most distinctly, a significantly higher frequency of V-shaped percussion cracks and craters (dominant on ca. 40% of Type 4 grains versus ca. 15% of Types 1–3). Other abrasion textures (fractures, steps, grooves) have a minor occurrence and are outnumbered by the remains of chemical alteration (mainly dissolution etching and pitting). As for Type 3, Type 4 sand surfaces typically reveal a weathered appearance.

In all but one sample quartz grains belonging to all four grain types can be distinguished (Fig. 5B). Type 3 particles dominate the sand assemblage in 11 of the 16 samples, with an occurrence between 12 and 64% (38% on average), followed by Type 1 grains that account for 0 to 53% (22% on average) of the quartz sands. Type 4 grains form the smallest sub-assemblage (5–44% with an average of 18%) but are nevertheless ubiquitous, as is Type 2 (8–38%; 22% on average). A high variability in grain-type abundance can be noted throughout the mound sequence. Although no systematic variation patterns emerge, the top seven samples all have a distinctly increased presence of Type 1 particles (36% mean), whereas the lower nine samples are relatively enriched in Type 3 (46% on average).

## 5. Discussion

### 5.1. Challenger Mound sediment contributors: provenance versus transport

#### 5.1.1. The coarse siliciclastic input into Challenger Mound

According to the microtextural analysis of the selected sand-sized quartz grains, the coarse siliciclastic matrix fraction suggests an association with the following processes.

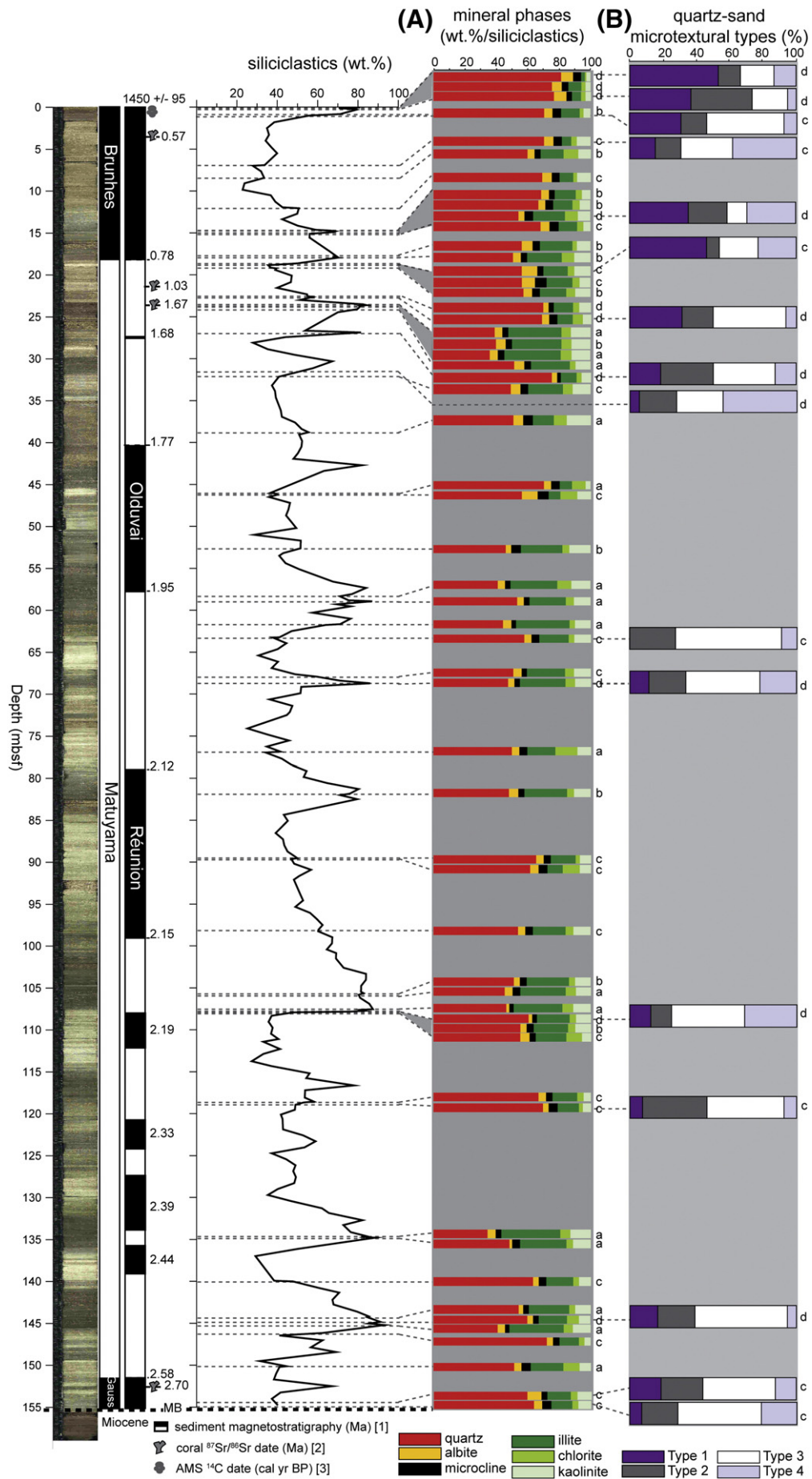
5.1.1.1. Type 1 grains: evidence for a significant ice-sheet influence. The features listed for Type 1 are the classic products of glacially-induced mechanical abrasion, related to transport by a substantial ice sheet (e.g. Mahaney and Kalm, 1995; Helland and Holmes, 1997; Mahaney and Kalm, 2000; Mahaney, 2002; Damiani et al., 2006; Eldrett et al., 2007; Cowan et al., 2008; St. John, 2008). The deep entrenchment of

conchoidal and linear fractures, their frequency of occurrence in combination with step features and (directional) grooves, the overall sharp angularity of grains and the absence of abundant V-shaped percussion cracks (Fig. 6A–B) clearly discriminate these glacially-abraded grains from those produced by impacts in other abrasive settings, such as high-energy subaqueous environments (Mahaney and Kalm, 2000; Mahaney et al., 2001; Mahaney, 2002). When glacial processes generate grain surfaces that are not this intensively abraded, identifying their glacial origin becomes less straight-forward (see Section 5.1.1.2). Therefore, Type 1 grains are considered a conservative, but confident estimate of quartz sand with a primary glacial/glacio-marine origin, most likely deposited in the close vicinity of the core site by melting icebergs. The limited amount of transport and redistribution in the marine environment is inferred from the lack of abundant V-shaped pits (see Section 5.1.1.3) and the generally very fresh and angular grain surfaces of the Type 1 sands (Fig. 6A–B) (cf. Strand et al., 2003; Damiani et al., 2006 for the Antarctic region). For all that, these V-shaped percussion cracks could be related to the influence of meltwater as to any other subaqueous medium, as shown by Cowan et al. (2008) and Mahaney (2002).

5.1.1.2. Types 2–3 grains: further indications of ice transport. Although largely similar, Type 2 sand surfaces cannot be as uniquely attributed to glacial abrasion as the Type 1 grains. The moderate intensity and frequency of the Type 2 mechanical abrasion features (Fig. 6C–D) might be induced during bedrock release, subaqueous transport as well as glacial abrasion (Ingersoll, 1974; Hill and Nadeau, 1984; Mahaney and Kalm, 2000; Mahaney, 2002). The low abundance of V-shaped pits and the angularity of the Type 2 grains (Fig. 6C–D), furthermore, imply limited subaqueous transport (see Section 5.1.1.3). Hence, besides a possible glacial-abrasion phase, dispersal in a low-energy, less abrasive subaqueous environment (Mahaney, 2002) can be inferred from Type 2 surfaces.

The Type 3 sub-rounded, predominantly etched (dissolution) outlines with little evidence of mechanical abrasion (Fig. 6E–F) are characteristically formed by subaerial or subaqueous silica dissolution (Crook, 1968; Higgs, 1979; Helland and Holmes, 1997; Mahaney, 2002; Damiani et al., 2006). Besides edge rounding no abrasion features are present to indicate significant subaqueous transport subsequent to this chemical weathering. Post-depositional, in situ silica dissolution, however, can be discarded, as the pore water pH remains around 7.3 for the whole Challenger Mound sequence (Ferdelman et al., 2006) and silica dissolution only takes place from pH 9 onwards. Moreover, in all samples different microtextural types are found together and not all quartz grains exhibit weathering features (e.g. Type 1 grains). Hence, quartz dissolution of light to moderate intensity (sensu Setlow, 1977) must have taken place prior to final deposition on Challenger Mound, either elsewhere in the marine environment or on land. It is intriguing as to how these sand-sized particles, dominant in most assemblages, could have been deposited onto Challenger Mound without substantial mechanical abrasion, bearing in mind it is an elevated structure experiencing enhanced current speeds (Dorschel et al., 2007) in an, at present, very dynamic benthic environment (Wheeler et al., 2007; White, 2007). One plausible scenario would be non-abrasive glacial transport directly onto or into the close vicinity of Challenger Mound. Damiani et al. (2006) and Cowan et al. (2008) described comparable, weathered grains in Antarctic marine cores and attributed their presence to supra- and/or englacial transport, in which grains can be more sheltered from abrasion than subglacially (Mahaney, 2002).

Fig. 5. X-ray diffraction phase quantification and quartz-sand microtextural results of selected Challenger Mound (U1317E) samples. Core position of samples (dashed lines) indicated on the total siliciclastic abundance plot (weight %) from Titschack et al. (2009). All depths in corrected metre below seafloor (mbsf); MB = mound base; [1] Foubert and Henriot (2009), [2] Kano et al. (2007) and [3] this study. (A.) Mineral quantification (weight %) of six phases in the siliciclastic fraction, per sample. (B.) Quantification (%) of four microtextural types (description in Fig. 6) in the quartz-sand assemblage, per sample. End-member dominance (a = EMA-dominated sample, etc.) per sample added for further reference (Figs. 7 and 8).



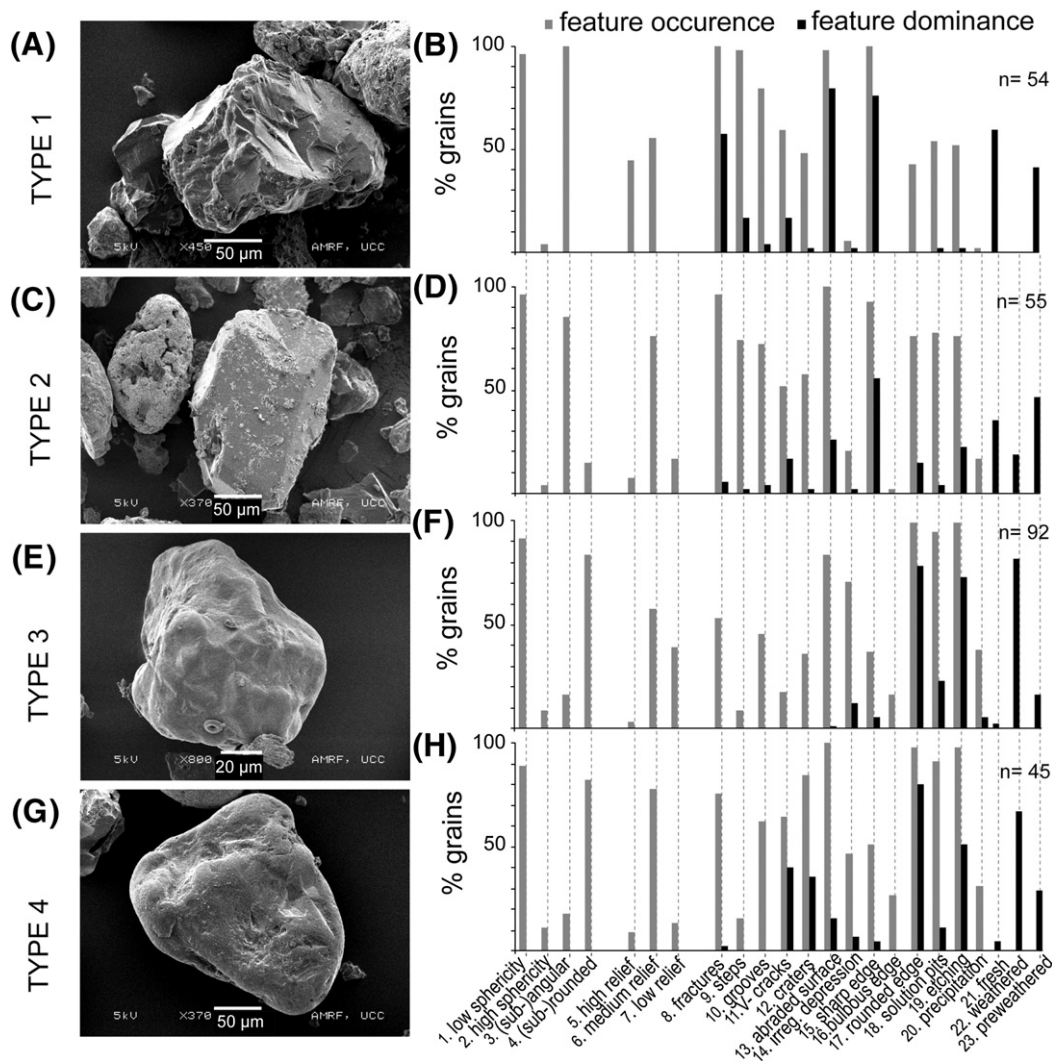


**Fig. 6.** Characterisation of Challenger Mound (U1317E) quartz-sand microtextural types. Scanning electron microphotographs of representative quartz grains belonging to the Type 1 (A), Type 2 (C), Type 3 (E) and Type 4 (G) grain types and frequency distributions (% grains per feature) of microtexture occurrence and dominance in each grain-type assemblage (B, D, F, H). *n* = number of grains analysed per grain type; surface features as defined in Table 2.

Closer to the study site similar deductions were made for “smooth grains” in the fine sand fraction of the North Atlantic Feni and Gardar drifts (Eggers and Ehrlich, 1985). Additionally, the incorporation of grains into sea ice may result in comparable surface features (St. John, 2008). Although a major process in the Arctic region, sea ice entrains mostly fine-grained sediments (Hebbeln, 2000; Dethleff and Kuhlmann, 2009) and is therefore not considered the dominant input source of Type 3 sand-sized grains. Consequently, also Type 3 (and potentially Type 2) microtextures suggest the importance of iceberg rafting as a depositional mechanism for the coarse fraction within Challenger Mound.

**5.1.1.3. Type 4 grains: limited evidence for intense current action.** The co-occurrence of a sub-rounded outline, multiple V-shaped percussion cracks and/or abrasion craters and a variety of chemical textures on Type 4 grains (Fig. 6G–H) can be attributed unambiguously to edge abrasion during high-energy subaqueous transport. Similar features have been reported from fluvial (Manker and Ponder, 1978; Mahaney and Kalm, 2000) and beach environments (Ingersoll, 1974), as well as from turbidite flows (Wang et al., 1982) and (bottom-) current action in the marine realm (Hill and Nadeau, 1984; Helland and Holmes, 1997; Strand et al., 2003; Damiani et al., 2006). Even grain-to-grain collisions in turbulent meltwater should not be excluded (Cowan

et al., 2008), especially considering the implied presence of melting ice in the vicinity of Challenger Mound (see previous sections).

In comparison to previously published subaqueous grains (e.g. Mahaney, 2002; Damiani et al., 2006), the Type 4 grains in this study are still fairly angular and not as heavily V-pitted. This suggests a relatively short residence time (most probably as suspension load) in this high-energy environment and/or a short transport distance to the site of final deposition. The ubiquitous presence of feldspar minerals (Fig. 5B), sensitive to both chemical and mechanical destruction, furthermore strengthens this interpretation. It therefore seems unlikely that this sub-assemblage has experienced prolonged reworking on the shelf or long-term transport by vigorous bottom-currents, which are established along the eastern North Atlantic continental margin (Weaver et al., 2000; White, 2007). Hence, if remobilised by bottom-currents, these sand-sized particles must be redistributed locally, with a local source area or a proximal deposition site after, e.g., non-abrasive glacial transport.

Considering the position of Challenger Mound on the eastern Porcupine Seabight slope, a valid alternative to (short distance) along-slope current transport could be down-slope sedimentation, as observed frequently along the eastern North Atlantic continental margin (e.g. Weaver et al., 2000). However, no sedimentary evidence is found in the Challenger Mound sequence nor in other sediment records in the BMP (Van Rooij et al., 2007; O'Donnell, pers.comm.;

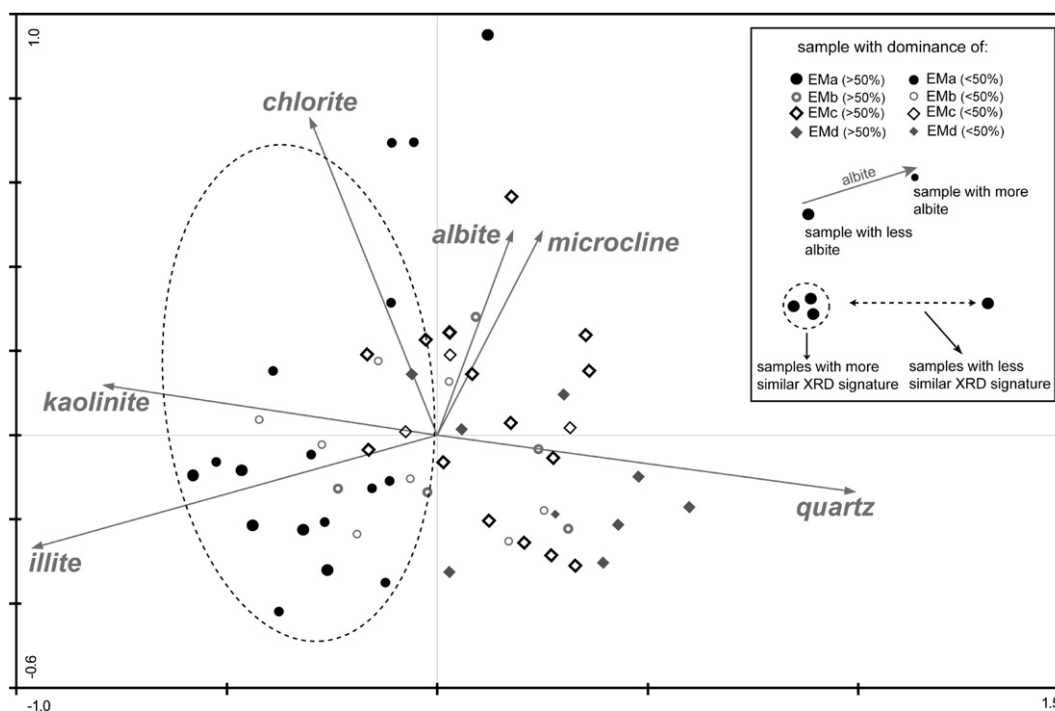


**Fig. 7.** Mineralogical characterisation of end-member-dominated lithofacies in Challenger Mound (U1317E). Principal Component Analysis (PCA) graph of X-ray diffraction (XRD) data illustrating the mineralogical (dis-)similarities of samples dominated by the different end-members (EM). Sample key and basic PCA plot principles explained in inset. Dashed circle points out the clay mineral (mainly illite and kaolinite) enrichment and clustering of EMa-dominated samples (black dots), indicating their mineralogical similarity and hydraulic relevance. Phase quantification data per sample in Fig. 5.

Huvenne et al., 2009b) for significant mass sediment transport (e.g. turbidites). It cannot be entirely excluded that sedimentary structures related to smaller-scale events are obscured in the record by bioturbation and/or sample resolution, or that finer-grained particles are derived from turbidity plumes. However, it is hard to envisage the deposition of sand-sized material from a turbidity plume onto the summit of a topographic elevation such as Challenger Mound. Therefore, if produced in the marine environment, Type 4 grain surfaces are proposed as indicators for limited, high-energy subaqueous transport by along-slope bottom-currents, unless the influx of meltwater is evident.

Overall, this microtextural study clearly identifies iceberg rafting as the prime input mechanism for the coarse-grained siliciclastic Challenger Mound fraction. In all selected samples, sand grains from an undisputable glacio-marine source (Type 1) and/or a strongly implied one (Types 2–3) have been distinguished and together comprise over 80% (average) of the assemblage (Fig. 5B). The primary origin of coarse material delivered to the Challenger Mound site, thus, appears invariable throughout its growth history. Besides this, remarkably little evidence is present for subaqueous transport (only significant in Type 4), indicating a minimal amount of resuspension and (re-)deposition of sands by bottom-currents, or even a lack thereof.

The wider context for, and further implications of these findings will be explored in the following sections.

### 5.1.2. Characterising sediment contributors

Through end-member modelling four significant elementary particle-size distributions (end-members (EM)) are distilled out of the total siliciclastic size dataset (Fig. 4). In this study, validation of actual end-member processes is focussed around the behaviour of end-members in “end-member-dominated” (EM-dominated) samples, enabling the characterisation of “EM-dominated lithofacies” (Figs. 6–8).

Importantly, particles with a distinct hydraulic equivalence tend to cluster together in separate EM-dominated samples (Fig. 7). Most

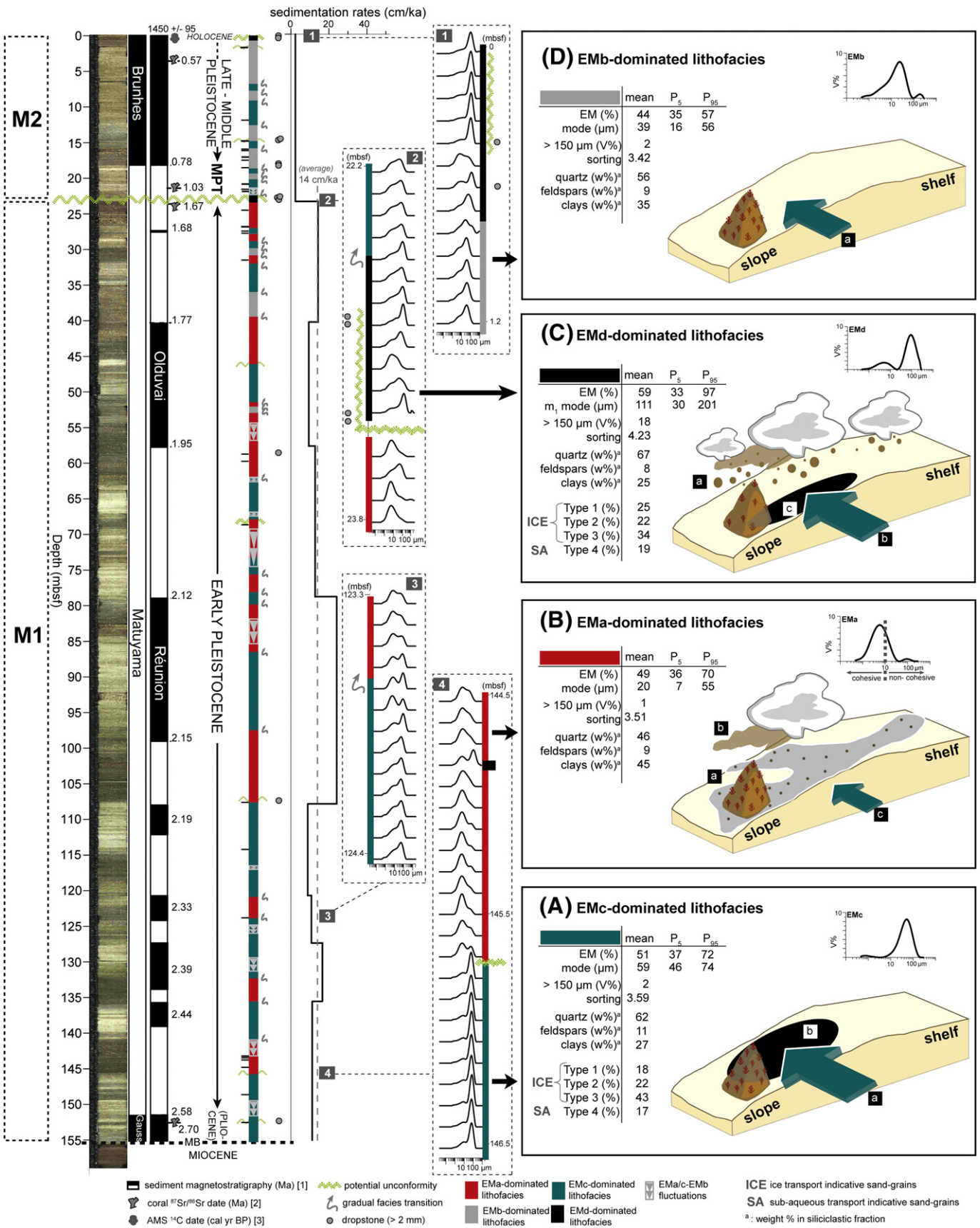
distinctly, EMa-dominated samples seem particularly enriched in clay minerals, who's specific habitat and cohesive properties (see Section 5.1.2.2) cause them to behave hydrodynamically different from quartz or feldspar grains, for example. The latter, on the other hand, are found dominating the mineralogy of especially EMc- and EMd-dominated samples (Fig. 7). The main assignment of clay minerals to the finest end-member (EMa) and the more robust, non-platy quartz and feldspars to the coarser ones (EMc–d) illustrates the hydrodynamic relevance of the EM-distributions. Moreover, the concentration of the clay fraction in the EMa size-range (Fig. 4A) resolves the issue of clay underestimation, which typically hinders reliable hydrodynamic reconstructions based on laser granulometry (see also Konert and Vandenberghe, 1997; McCave and Hall, 2006). The end-member modelling approach thus allows for a meaningful hydrodynamic interpretation of the Challenger Mound siliciclastic laser particle-size data.

**5.1.2.1. EMc-dominated lithofacies.** The particle-size signature of the most dominant end-member, EMc, with a leptokurtic distribution relatively sorted around a coarse silt-size mode and a significant tail towards the finer fractions (Fig. 4A), clearly indicates a current influence. The EMc-dominated lithofacies (Fig. 8A) is, therefore, a current-controlled, residual facies (sensu Michels, 2000), typically associated with the sorting action of contour-currents. These are capable of transporting and depositing non-cohesive, coarser-grained particles while suppressing the deposition of fines. In a non-coral carbonate mound context EMc-dominated sediments would be described as silty contourites (sensu Stow et al., 2002), as in addition to the current-sorting signal no primary structures are recognised and homogenising bioturbation is ubiquitous.

Whether bottom-currents are sorting sediment while actively depositing material or merely winnowing/resuspending sediments syn-/post-depositional, needs consideration as it will determine further hydrodynamic inferences. Coarse fraction microtextural analysis (Figs. 5B and 8A) reveals that even in EMc-dominated samples only a

minor grain-assembly carries a potential current-transport signal (Type 4 grains, with average abundance of 17% in EMc-dominated samples) whereas most quartz-sand surfaces suggest ice-related

transport without an intense subaqueous influence (Type1–3; Fig. 8A). It has been suggested by McCave and Hall (2006) that sufficiently strong currents are able to sort ice-rafted sediments syn-depositionally, hence



superimposing a current-sorted size-signal on a non-sorted ice-rafted distribution. This would, however, require the concurrent presence of both ice-rafting and sufficient contour-current strength, repeatedly and for significant periods of time throughout mound development (Fig. 8). At least for the Late Pleistocene, ice-rafting has only been associated with reduced bottom-current activity in the area (Hall and McCave, 2000; Øvrebø et al., 2006; Rüggeberg et al., 2007; Van Rooij et al., 2007), which questions this hypothesis. Alternatively, material originally emplaced by melting ice, is at a later stage resuspended (by peak bottom-currents or tidal waves, for example) and entrained by along-slope currents. The latter then transport, sort and finally redeposit the material and in this way actively contribute to the sediment accumulation on Challenger Mound. As implied by the microtextural analysis (Section 5.1.1), the subaqueous redistribution of sand-sized material must have been limited. Therefore, short-distance, suspension load transport from the close-by Irish continental shelf/slope or elsewhere on Challenger Mound itself is proposed. Current intensities, flow regimes and hence sedimentation patterns can vary significantly between different areas on coral carbonate mounds (e.g. flanks versus summit; Dorschel et al., 2007). Hence, very local resuspension and redeposition of mound sediments would make a reasonable, local source for coarse-grained material without substantial, current-induced mechanical abrasion. The depositional history of the silt-size-fraction is assumed at least partly similar to that of the sand fraction, although it cannot be excluded that additional processes potentially influenced the silt fraction prior to dispersal by contour-currents.

In order to deposit sediments with a modal size between 74 and 46  $\mu\text{m}$  (i.e. 90% of samples in the EMc-dominated facies; Fig. 8A) from suspension, current speeds need to drop below 9.1 (for 74  $\mu\text{m}$ ) to 3.7  $\text{cm s}^{-1}$  (for 46  $\mu\text{m}$ ; at 1 m above the seabed; calculated according to the methodology of Huvenne et al. (2009a), with water-mass data from Dorschel et al. (2009) and Klages et al. (2004)). Critical resuspension thresholds for the same sediment lay between 32.7 and 30.7  $\text{cm s}^{-1}$ . A significant reduction in current strength is thus required after initial (peak current) resuspension, considering the implied, short transport distance of the sediment and the current acceleration induced by the mound topography itself (Dorschel et al., 2007). As suggested for a similar facies in U1317C by Huvenne et al. (2009b) and quantified by Duineveld et al. (2007) and Mienis et al. (2009) in the Rockall area, the prime mechanism for lowering current speeds on coral carbonate mounds, besides slack tidal periods, is a (dense) coral cover. Moreover, the coral framework dampens the effect of sediment resuspension and favours sediment preservation and accumulation at mound sites (Mienis et al., 2009).

Overall, EMc-dominated sediment accumulation on Challenger Mound originates from the balanced interplay between 1) contour-currents capable of predominantly local and relatively energetic sediment transport and 2) a cold-water coral cover promoting current speed reduction below ca. 9  $\text{cm s}^{-1}$  and hence, facilitating sediment deposition and preservation (Fig. 8A).

**5.1.2.2. EMa-dominated lithofacies.** The second most abundant lithofacies is dominated by the poorly sorted EMa-distribution with its fine

silt-size mode (ca. 6  $\mu\text{m}$ ) and over 78% of particles smaller than 10  $\mu\text{m}$  (Figs. 4A and 8B). This 10  $\mu\text{m}$  size-limit is of great importance as it demarcates non-cohesive (>10  $\mu\text{m}$ ) from cohesive (<10  $\mu\text{m}$ ) particle behaviour, inducing single grain (>10  $\mu\text{m}$ ) versus aggregated (<10  $\mu\text{m}$ ) dispersal (McCave et al., 1995; Chang et al., 2007). Therefore, sediments predominantly consisting of small (<10  $\mu\text{m}$ ) clay particles (cf. EMa-dominated samples; Figs. 7 and 8B), were transported and deposited as aggregates (i.e. particles bound together by biological and/or physical processes). Hydrodynamic inferences from aggregates are not straight-forward as they behave hydraulically equivalent to the coarser, non-cohesive grains that were deposited concurrently (Chang et al., 2007). Overall, aggregate-rich deposits do suggest a relatively quiescent environment, at least periodically (Fig. 8B), as aggregate break-up in more energetic conditions would significantly suppress the deposition of fines (McCave and Hall, 2006). This is the case in the EMc-dominated environment, where EMa contributions are still present, although to a lesser extent (Fig. 4B). Once deposited, dismantling of aggregates is most likely (Chang et al., 2007) and resuspension imminent, unless a sediment preserving agent exists. The presence of a dense, stabilising coral framework, therefore, would significantly promote accumulation of the EMa-dominated lithofacies.

At present, an easy-erodible layer of aggregated particles is identified in several slope locations along the west European continental margin, e.g. at the nearby Goban Spur (Fig. 1) (Thomsen and Gust, 2000). The entrainment of resuspended shelf/slope sediment into bottom and intermediate nepheloid layers and the subsequent rain-out of aggregates that formed in these nepheloid clouds (Fig. 8B), is a major input process of particulate and fine siliclastic material in the region (McCave et al., 2001; van Weering et al., 2001). It is also responsible for the supply of fresh food particles to cold-water coral sites (Mienis et al., 2007). Additionally, Knutz et al. (2002) propose deposition from meltwater plumes for a Late Pleistocene fine lithofacies on the Barra Fan, due to the association of the fine sediment with scattered, more sandy intervals and ice-rafted debris. This process may also be of relevance for the EMa-dominated lithofacies, as repeatedly in these deposits coarser, EMd-dominated horizons and mm- to cm-size lithics (dropstones) are found (Fig. 8; see Section 5.1.2.3).

Aggregated fines, therefore, may have been available in several ways throughout mound development and, irrespective of their origin, account for a considerable part of the Challenger Mound sediment sequence (Fig. 8).

**5.1.2.3. EMd-dominated lithofacies.** Downcore, distinct horizons (usually spanning only 1 sample interval) with an EMd-dominance are present. Their bimodal, poorly sorted and coarser particle-size signature, especially enriched in sand-sized grains larger than 150  $\mu\text{m}$  (18% versus 1–2% for the other EM-facies; Figs. 4A and 8C), is generally attributed to non-size-selective ice-rafting processes, particularly in this part of the NE Atlantic (Bond et al., 1992; Prins et al., 2002; Peck et al., 2007; Van Rooij et al., 2007 and references therein). The quartz-sand microtextural analysis decisively supports the ice-rafted origin of the coarse EMd-fraction (Figs. 5B and 8C). Moreover, the combination of fresh glacially-

**Fig. 8.** Challenger Mound (U1317E) sediment contributors and hydrodynamic environments. The downcore alternation of end-member (EM)-dominated lithofacies is visualised, illustrating the clear shift in sedimentary environment between the lower mound-phase (M1) and upper mound-phase (M2). Examples of typical particle-size spectra (0.01–2000  $\mu\text{m}$ ; logarithmic scale) from four depth intervals (1–4) further document the four lithofacies and their transitions throughout the mound sequence. All depths in corrected metre below seafloor (mbsf); MB = mound base; MPT = mid-Pleistocene climate transition; [1] Foubert and Henriët (2009), [2] Kano et al. (2007) and [3] this study; sedimentation rates based on [1] and [3]; average sedimentation rate for M1 (grey dashed line). (A.) Characterisation of EMc-dominated lithofacies and its proposed depositional environment. Higher-energy contour-currents (a) transport and redeposit mainly locally-derived sediments (b) on a densely coral-covered Challenger Mound. (B.) Characterisation of EMa-dominated lithofacies and its proposed depositional environment. Aggregate deposition from shelf/slope-derived nepheloid layers (a) or iceberg meltwater plumes (b) occurs in a more quiescent environment influenced by (periodically) less energetic bottom-currents (c). A sufficiently dense coral cover facilitates preservation of these finer-grained deposits. (C.) Characterisation of EMd-dominated lithofacies and its proposed depositional environment. In situ deposition of iceberg-rafted material (a) occurs, at times followed by post-depositional current-winnowing (b). Deposition of locally-derived material (c) during peak current events (b) cannot be excluded for certain EMd-dominated horizons. (D.) Characterisation of EMb-dominated lithofacies and its proposed depositional environment. Deposition and (re-)suspension of sediment occurs in a current-controlled environment energetically intermediate (a) compared to the environments inferred in (A.) and (B.). See text for more detailed descriptions.

abraded grains (Type 1; on average 25% of assemblages, with peaks up to 53%; Fig. 5B) with the poorly sorted, coarse particle-size signature of EMD-dominated sediments (Fig. 8C), further supports deposition from icebergs rather than sea ice (Hebbeln, 2000; Dethleff and Kuhlmann, 2009). Notably, very similar microtextural assemblages are reported for the bottom-current-reworked EMC-quartz sands and independently, the microtextural study does not allow the discrimination between EMC- and EMD-dominated samples (Fig. 5B). Most EMD-dominated particle-size distributions, however, do not show any evidence of a considerable current influence and even correlate to distinct drops in sediment sorting (Figs. 3 and 8C). The enrichment of coarse particles is, therefore, not produced by selective winnowing/deposition, but rather by the input of a particle-size continuum.

The unimodal appearance and associated size-sorting of certain EMD-dominated distributions (e.g. top samples; Fig. 8) could originate from post-depositional exposure of ice-rafted material to winnowing bottom-currents. However, the data cannot exclude that peak current events (erosion threshold  $>33 \text{ cm s}^{-1}$  for  $100 \mu\text{m}$  mode sediments) were able to locally mobilise and deposit these coarse particles similarly to EMC-dominated deposits. Nevertheless, in situ emplacement of discrete, ice-rafted deposits is generally proposed for EMD-dominated samples (Fig. 8C).

**5.1.2.4. Emb-dominated lithofacies.** The mesokurtic particle-size distributions (mean  $39 \mu\text{m}$  mode) of the Emb-dominated samples, in general better sorted than averagely (Fig. 8D), suggest a repeatedly current-influenced depositional environment (Michels, 2000), energetically intermediate between the inferred EMC- and EMA-dominated environments. The intermediate nature of Emb-dominated samples is also reflected in a variable, mixed mineral assemblage, as expected for the Emb size-range (Figs. 7 and 8D).

Emb dominates the assemblage of 20% of Challenger Mound samples, while its presence is significant (min. 10% abundance) in 84% of EMC- or EMA-dominated samples (Fig. 4B). As a medium-silt-dominated sediment mixture, in comparison to cohesive clay/fine silt (EMA) and coarser silt (EMC) fractions, can more easily be resuspended/non-deposited ( $39 \mu\text{m}$ : critical settling velocity below  $3 \text{ cm s}^{-1}$ , resuspension threshold of ca.  $30 \text{ cm s}^{-1}$ ), the varying abundance of Emb may result from subtle shifts in the energetic mode of the controlling bottom-current. Bearing in mind the basic EMMA assumption of a constant-sum (100%) mixing of non-negative end-members with fixed compositions (Weltje, 1997), this end-member probably is a product of the method and actually emanates from the variable current system responsible for the EMC- versus EMA-dominated sediments, rather than a separate input process (Fig. 8D).

## 5.2. Challenger Mound depositional sequence: hydrodynamic environments

The particle-size end-member analysis, XRD siliciclastic quantification and quartz-sand microtextural datasets all agree on a clear change in sediment properties of the mound sections above and below ca. 23 mbsf (Figs. 4B and 5). The sudden and distinct shift towards coarser, more quartz-rich sediments exhibiting abundant glacially-abraded quartz-sand surfaces (Type 1) (0–23.4 mbsf; Figs. 3, 4B and 5), clearly coincides with the Kano et al. (2007) hiatus in the *Lophelia pertusa*  $^{87}\text{Sr}/^{86}\text{Sr}$  stratigraphic record for Challenger Mound (Fig. 8). This “mound crisis” event (Titschack et al., 2009), thus not only affected coral growth but also on-mound sedimentation and accordingly, our study supports a two-phase mound development.

### 5.2.1. The lower mound-phase (M1): 2.6–1.7 Ma

The ca. 132 m thick lower mound-phase (M1) is characterised by the repetitive alternation of the coarser EMC- and finer EMA-dominated lithofacies, reflecting respectively the higher and lower energetic modes of the governing contour-current system (Fig. 8). As EMA-dominated sediments only occur in M1, while coarser sediments dominate the upper mound sections, we propose the boundary

between the uppermost EMA-dominated interval and the overlying EMD-dominated horizon, at 23.4 mbsf, as the sedimentological demarcation of the two mound phases (Fig. 8).

Sediment accumulation in the U1317E site initiated under the relatively higher-energetic current-controlled environment implied for EMC-dominated deposits, which compares to findings of Huvenne et al. (2009b) for sedimentation start-up in the parallel hole U1317C. Although the basal deposits of this mound site are assumed to be slightly younger (ca. 2.4–2.1 Ma in U1317C (Huvenne et al., 2009b) versus ca. 2.6 Ma in U1317E (Foubert and Henriot, 2009)), comparable hydrodynamic conditions facilitated initial sediment accumulation at both Challenger Mound sites. Deposition of the first U1317E mound facies (average modal sizes of  $56 \mu\text{m}$ ; Fig. 3) required minimum resuspension speeds of  $31.6 \text{ cm s}^{-1}$ , subsequently slowed down below  $5.5 \text{ cm s}^{-1}$  (cf. Section 5.1.2.1). Transitions between EMC- and EMA-dominated deposits are generally gradual and smoothed by bioturbation (Fig. 8). As energetic differences between both facies are often subtle, M1 seems to attest to a rather continuous, steadily changing, current-controlled depositional environment. Only rarely are sediment transitions abrupt and suggest the presence of potential unconformities, although the latter cannot be confirmed due to the limited resolution of the existing stratigraphic models (Fig. 8). Similarly, individual facies sedimentation rates cannot be determined at present, but average accumulation rates of ca.  $14 \text{ cm ka}^{-1}$  (based on Foubert and Henriot, 2009) illustrate the fast sediment built-up during this first mound development stage. The confined hydrodynamic variability during M1 might be the expression of the general Early-Pleistocene climate system (cf. Sakai et al., 2009; Titschack et al., 2009). Climatic variability was less extreme in the 41-ka-orbitally-dominated Early-Pleistocene compared to the 100-ka-paced Mid-Late Pleistocene (Lisiecki and Raymo, 2005; Sosdian and Rosenthal, 2009). Climatically-steered fluctuations in ocean circulation, ice volume and/or eustatic sea-level could therefore have affected the Challenger Mound environment, without exceeding its threshold conditions. Overall, the Early-Pleistocene environment appears favourable for fast and semi-continuous mound growth, which equally implies the (semi-) continuous presence of a sufficiently dense coral framework. As discussed above, sediment deposition and preservation, especially in a repeatedly varying current-driven environment, greatly benefit from the sediment-stabilising capacity of a dense coral cover. The lack of M1-equivalent off-mound deposits in the neighbouring U1318 site (Fig. 1) (Huvenne et al., 2009b; O'Donnell, pers. comm.; Titschack et al., 2009) illustrates the poor preservation potential of sedimentary deposits in a dynamic continental margin setting without additional, sediment-stabilising agent. Even regionally, the Challenger Mound M1 sequence presents a unique, (Plio-)Pleistocene sedimentary record, as during this time period erosion/non-deposition prevailed along most of the NW European continental margin (Van Rooij et al., 2003; Laberg et al., 2005).

Notably, ice-rafted grains are most common constituents of the M1 sand fraction, predominantly deposited by locally resuspending bottom-currents (EMC-dominated lithofacies), although in situ ice-rafted horizons (EMD-dominated lithofacies) are identified as well (Figs. 5B and 8). Even in the basal Challenger Mound sediments, dated around 2.6 Ma (Foubert and Henriot, 2009), (reworked) glacial grains are frequent (Fig. 5B). This would suggest that even in the early stages of large-scale Northern Hemisphere ice-sheet expansion (ca. 2.74–2.4 Ma; Shackleton et al., 1984; Maslin et al., 1996; Jansen et al., 2000) ice extended sufficiently offshore to release calving icebergs, which repeatedly reached as far south-east as the eastern Porcupine Seabight continental margin. By that time, surges from ice sheets on Greenland, Iceland and Scandinavia released ice-rafted detritus into the North Atlantic Ocean (e.g. Helland and Holmes, 1997; Jansen et al., 2000; Flesche Kleiven et al., 2002). However, any provenance determination remains speculative without further analyses. Irrespective of origin, iceberg rafting proves important as sediment supplying mechanism even throughout the M1 development phase of Challenger Mound.

Sedimentologically there is little evidence in the M1 sequence announcing the environmental switch leading to its abrupt ending (Fig. 8).

### 5.2.2. The upper mound-phase (M2): 998–1.5 ka

In the ca. 23 m thick upper mound-phase (M2), generally coarser sediments accumulate at significantly reduced rates (ca.  $2 \text{ cm ka}^{-1}$  average, based on Foubert and Henriet (2009) and this study's  $^{14}\text{C}$  AMS date) (Fig. 8). Alternating EMc- and EMb-dominated lithofacies still provide evidence for sediment deposition by a fluctuating contour-current system, although fine, cohesive sediment accumulation (EMa-dominated) seems replaced by a more intermediate, non-cohesive (EMb-dominated) one. Therefore, the M2 current-controlled environment appears overall more energetic than the one described for M1 (Fig. 8). Syn-/post-depositional peak current events and associated unconformities are potentially located where the coarse EMd-dominated horizons occur, as illustrated especially in both the top and bottom ca. 0.6 m of M2 (Fig. 8). Considering the fine silt accumulation off-mound, at least partly synchronous with M2 deposition (Huvenne et al., 2009b; O'Donnell, pers. comm.), the slow accumulation of mostly coarse silt and sand deposits on Challenger Mound seems to result from a reduced capacity to deposit and/or preserve finer-grained material on the mound rather than from an absence of fines in the environment. As the elevation of a mound structure induces current acceleration (Dorschel et al., 2007), the overall coarser deposits on-mound versus off-mound can be attributed to mound topography. However, increasing mound height alone cannot explain the hydrodynamic difference between M1 and M2, as no systematic change in sediment properties can be discerned with mound height during its rapid, ca. 132 m growth in M1 (Fig. 8). It is hard to envisage how its moderate additional growth suddenly would have a determining impact on sediment dynamics. The position of the mound in relation to the surrounding water masses, on the other hand, can significantly influence coral growth, as e.g. optimal current speed and food supply conditions occur at the density gradient between water masses (Freiwald, 2002; White et al., 2007). Deviation from these optimal conditions may result in reduced coral density, which in turn hampers sediment deposition and preservation, enabling the observed depositional shift to a coarser, condensed M2 sequence. Due to the complexity of the coral-quantity variation (Titschack et al., 2009), Challenger Mound coral and matrix sediment records cannot be adequately integrated at present to conclusively validate this hypothesis.

The Challenger Mound sand fraction, furthermore, holds proof of a significant glacial advance. The general increase in glacially-abraded quartz grains in M2 (Fig. 5B: Type 1 grains 36% mean abundance in M2 versus 11% in M1) strongly suggests a more proximal ice source, actively influencing the study site (e.g. Strand et al., 2003). These findings and their timing (ca. 998 ka for M2 basal sediment; Foubert and Henriet, 2009), fit well into the global pattern of the mid-Pleistocene climate transition, associated with a marked increase in global ice volume (at ca. 1–0.9 Ma), followed by an abrupt change in the periodicity and amplitude of climate cycles (at ca. 700–650 ka) (e.g. Mudelsee and Statterger, 1997; Helmke et al., 2005). A sharpened contrast between climatic extremes, intense proximal glaciation and higher amplitude global sea-level fluctuations (e.g. Sosdian and Rosenthal, 2009) result from this transition and all have the potential to alter coral growth and sediment accumulation, hence affecting mound development. The observed shift from M1 to M2 is, therefore, most likely the expression of the global climatic and oceanographic rearrangements during the mid-Pleistocene (cf. Kano et al., 2007; Huvenne et al., 2009b; Sakai et al., 2009; Titschack et al., 2009). Overall, it seems that the two major climate transitions of the Plio-Pleistocene, i.e. the onset of Northern Hemisphere glaciation (ca. 2.7–2.4 Ma) and the mid-Pleistocene climate transition (ca. 1 Ma–650 ka), indicate two major thresholds in mound development: mound initiation (M1) and mound decline (M2).

The coarse ( $>120 \mu\text{m}$  mode), quartz-rich and current-sorted sediments at the top of the mound sequence (Figs. 5 and 8) illustrate the recent high-energy sedimentary environment, in which sediment accumulation is minimal and no new phase of coral growth is observed.

## 6. Conclusions

- The Challenger Mound deposits, rather than being determined by sediment input, seem defined by the strength of re-dispersal in the marine environment. Evidence for the influence of an all dominant contour-current system, operating in variable energetic modes, is omnipresent. Besides, the coarse-grained siliciclastic fraction clearly identifies iceberg rafting as its prime, initial depositional mechanism.
- Initial deposition of glacially-transported grains is suggested proximal to the study site, as remarkably little evidence for significant subaqueous resuspension and (re-)deposition of sands is present. Only local, short-distance bottom-current transport is therefore proposed. The deposition of ice-rafted detritus appears important as sediment supplying mechanism throughout the entire mound development period. Evidence for icebergs repeatedly reaching as far south-east as the eastern Porcupine Seabight continental margin, even in the early stages of Northern Hemisphere glacial expansion, is preserved in the mound sequence.
- In accordance to the proposed stratigraphic models, the Challenger Mound depositional sequence evidences a two-phase mound development. The lower mound-phase (M1; 2.6–1.7 Ma) suggests a semi-continuous, steadily changing, fast accumulating current-controlled depositional environment. The condensed upper mound-phase (M2; 998–1.5 ka), on the other hand, signifies a distinct and sudden shift to a more glacially-influenced, low accumulation setting. This shift results most likely from a reduced capacity to deposit and/or preserve sediments in the dynamic environment of an elevated structure exposed to the more extremely varying global environment since the mid-Pleistocene climate transition.
- Considering the variability and strength of the implied hydrodynamic environment, the sediment-stabilising and current-reducing capacities of a dense coral cover appear essential in promoting sediment deposition and preservation on Challenger Mound. We believe the presence of such an optimal coral cover responsible for the fast M1 development phase of Challenger Mound. It also facilitated sediment accumulation on-mound in the general erosive/non-depositional Early-Pleistocene environment along the NE Atlantic continental margin. A unique, higher resolution record is therefore preserved in the lower M1 sequence, illustrating the potential of cold-water coral carbonate mounds as intermediate water depth, continental margin, (Plio-)Pleistocene palaeo-archives.

## Acknowledgments

The authors would gratefully like to acknowledge the IODP Exp. 307 shipboard crew and scientists for providing this study's scientific framework and core material. Special thanks to W. Hale and A. Wülbers at the IODP core repository (Bremen) for repeated help with sample collection, to G.J. Weltje (Technical University Delft) for kindly providing the end-member modelling algorithm and to M. Cotter and S. Crotty at the Electron Microscopy Facility (BioScience Institute, University College Cork) for enthusiastic assistance with preparing and imaging specimen for this study. H. Pirllet (Universiteit Gent) is greatly thanked for numerous inspiring Challenger Mound discussions. We are also most grateful to D.J.W. Piper, J.S. Laberg and one anonymous reviewer for their comments, which greatly helped to improve this document.

This research was funded by the Marine Institute of Ireland, with the support of the Geological Survey of Ireland.

## References

- Belderson, R.H., Kenyon, N.H., Wilson, J.B., 1973. Iceberg plough marks in the Northeast Atlantic. *Palaeogeography, Palaeoclimatology, Palaeoecology* 13, 215–224.
- Beyer, A., Schenke, H.W., Klenke, M., Niederjaspser, F., 2003. High resolution bathymetry of the eastern slope of the Porcupine Seabight. *Marine Geology* 198, 27–54.
- Blott, S.J., Pye, K., 2001. GRADISTAT: a grain size distribution and statistics package for the analysis of unconsolidated sediments. *Earth Surface Processes and Landforms* 26, 1237–1248.
- Bond, G., Heinrich, H., Broecker, W., Labeyrie, L., McManus, J., Andrews, J., Huon, S., Jantschik, R., Clasen, S., Simet, C., Tedesco, K., Klas, M., Bonani, G., Ivy, S., 1992. Evidence for massive discharges of icebergs into the North Atlantic ocean during the last glacial period. *Nature* 360, 245–249.
- Cater, J.M.L., 1987. An application of scanning electron microscopy of quartz sand surface textures to the environmental diagnosis of Neogene carbonate sediments, Finestrat Basin, south-east Spain. *Sedimentology* 31, 717–731.
- Chang, T.S., Flemming, B.W., Bartholoma, A., 2007. Distinction between sortable silts and aggregated particles in muddy intertidal sediments of the East Frisian Wadden Sea, southern North Sea. *Sedimentary Geology* 202, 453–463.
- Cheary, R.W., Coelho, A., 1992. A fundamental parameters approach to X-ray line-profile fitting. *Journal of Applied Crystallography* 25, 109–121.
- Cheary, R.W., Coelho, A.A., Cline, J.P., 2004. Fundamental parameters line profile fitting in laboratory diffractometers. *Journal of Research on the National Institute of Standards and Technology* 109, 1–25.
- Cowan, E.A., Hillenbrand, C.-D., Hassler, L.E., Ake, M.T., 2008. Coarse-grained terrigenous sediment deposition on continental rise drifts: a record of Pliocene–Pleistocene glaciation on the Antarctic Peninsula. *Palaeogeography, Palaeoclimatology, Palaeoecology* 265, 275–291.
- Crook, K.A.W., 1968. Weathering and roundness of quartz sand grains. *Sedimentology* 11, 171–182.
- Damiani, D., Giorgetti, G., Turbanti, I.M., 2006. Clay mineral fluctuations and surface textural analysis of quartz grains in Pliocene–Quaternary marine sediments from Wilkes Land continental rise (East-Antarctica): paleoenvironmental significance. *Marine Geology* 226, 281–295.
- De Mol, B., Van Rensbergen, P., Pillen, S., Van Herreweghe, K., Van Rooij, D., Huvenne, V.A.I., McDonnell, A., Ivanov, M., Swennen, R., Henriot, J.P., 2002. Large deep-water coral banks in the Porcupine Basin, southwest of Ireland. *Marine Geology* 188, 193–231.
- De Mol, B., Kozachenko, M., Wheeler, A.J., Alvares, H., Henriot, J.P., Olu- Le Roy, K., 2007. Thérèse Mound: a case study of coral bank development in the Belgica Mound Province, Porcupine Seabight. *International Journal of Earth Sciences* 96, 103–120.
- Dethleff, D., Kuhlmann, G., 2009. Entrainment of fine-grained surface deposits into new ice in the southwestern Kara Sea, Siberian Arctic. *Continental Shelf Research* 29, 691–701.
- Dickson, R.R., McCave, I.N., 1986. Nepheloid layers on the continental slope west of Porcupine Bank. *Deep-Sea Research* 33, 791–818.
- Dorschel, B., Hebbeln, D., Rüggeberg, A., Dullo, W.-C., Freiwald, A., 2005. Growth and erosion of a cold-water coral covered carbonate mound in the Northeast Atlantic during the Late Pleistocene and Holocene. *Earth and Planetary Science Letters* 233, 33–44.
- Dorschel, B., Hebbeln, D., Foubert, A., White, M., Wheeler, A.J., 2007. Hydrodynamics and cold-water coral facies distribution related to recent sedimentary processes at Galway Mound west of Ireland. *Marine Geology* 244, 184–195.
- Dorschel, B., Coughlan, M., Crowe, B., de Clive-Lowe, E., Jackson, S., Joshi, S., O'Donnell, R., Ryan, C., Thierens, M., Wolff, C., Wheeler, A.J., 2009. Report of the CELTIC EXPLORER Cruise CE0907 with the Holland I Marine Institute Remotely Operated Vehicle (ROV) to the Belgica Mound province, eastern Porcupine Seabight. *Marine Institute Internal Reports*. 29 pp.
- Dowdeswell, J.A., 1982. Scanning electron-micrographs of quartz sand grains from cold environments examined using Fourier shape-analysis. *Journal of Sedimentary Petrology* 52, 1315–1323.
- Dowdeswell, J.A., Osterman, L.E., Andrews, J.T., 1985. Quartz sand grain shape and other criteria used to distinguish glacial and non-glacial events in a marine core from Frobisher Bay, Baffin Island, N.W.T., Canada. *Sedimentology* 32, 119–132.
- Duineveld, G., Lavaley, M.S.S., Bergman, M.J.N., de Stigter, H.C., Mienis, F., 2007. Trophic structure of a cold-water coral mound community (Rockall Bank, NE Atlantic) in relation to the near-bottom particle supply and current regime. *Bulletin of Marine Science* 81, 449–467.
- Dullo, W.-C., Flögel, S., Rüggeberg, A., 2008. Cold-water coral growth in relation to the hydrography of the Celtic and Nordic European continental margin. *Marine Ecology – Progress Series* 371, 165–176.
- Eggers, M.R., Ehrlich, R., 1985. Provenance Changes of Fine Quartz Sands in Glacial and Interglacial Intervals of the Feni and Gardar Drifts, North Atlantic: Fourier Shape Analysis. *DSDP leg 94*.
- Eldrett, J.S., Harding, I.C., Wilson, P.A., Butler, E., Roberts, A.P., 2007. Continental ice in Greenland during the Eocene and Oligocene. *Nature* 446, 176–179.
- Ferdelman, T.G., Kano, A., Williams, T., Henriot, J.P., IODP Exp. 307 Scientists, 2006. Proceedings of the IODP Expedition 307. Modern Carbonate Mounds: Porcupine Drilling. IODP Management International, Washington DC. doi:10.2204/iodp.proc.307.2006.
- Flesche Kleiven, H., Jansen, E., Fronval, T., Smith, T.M., 2002. Intensification of Northern Hemisphere glaciations in the circum Atlantic region (3.5–2.4 Ma) – ice-rafted detritus evidence. *Palaeogeography, Palaeoclimatology, Palaeoecology* 184, 213–223.
- Folk, R.L., Ward, W.C., 1957. Brazos River Bar: a study in the significance of grain size parameters. *Journal of Sedimentary Petrology* 27, 3–26.
- Foubert, A., Henriot, J.P., 2009. Nature and Significance of the Recent Carbonate Mound Record: the Mound Challenger Code. Springer-Verlag, Heidelberg. 350 pp.
- Foubert, A., Van Rooij, D., Blamart, D., Henriot, J.P., 2007. X-ray imagery and physical core logging as a proxy of the content of sediment cores in cold-water coral mound provinces: a case study from Porcupine Seabight, SW of Ireland. *International Journal of Earth Sciences* 96, 141–158.
- Freiwald, A., 2002. Reef-forming cold-water corals. In: Wefer, G., Billet, D.S.M., Hebbeln, D., Jørgensen, B.B., Schlüter, M., van Weering, T.C.E. (Eds.), *Ocean Margin Systems*. Springer-Verlag, Berlin, pp. 365–385.
- Frenz, M., Hoppner, R., Stuut, J.-B.W., Wagner, T., Henrich, R., 2003. Surface sediment bulk geochemistry and grain-size composition related to the oceanic circulation along the South American continental margin in the Southwest Atlantic. In: Wefer, G., Mulitza, S., Ratmeyer, V. (Eds.), *The South Atlantic in the Late Quaternary: Reconstruction of Material Budgets and Current Systems*. Springer-Verlag, Berlin, pp. 347–373.
- Games, K.P., 2001. Evidence of shallow gas above the Connemara oil accumulation, Block 26/28, Porcupine Basin. In: Shannon, P.M., Haughton, P.D.W., Corcoran, D.V. (Eds.), *The Petroleum Exploration of Ireland's Offshore Basins: Geological Society of London, Special Publication*, pp. 361–373.
- GEBCO, 2003. GEBCO Digital Atlas: Centenary Edition of the IHO/IOC General Bathymetric Chart of the Oceans. British Oceanographic Data Centre, Liverpool.
- Hall, I.R., McCave, I.N., 2000. Palaeocurrent reconstruction, sediment and thorium focussing on the Iberian margin over the last 140 ka. *Earth and Planetary Science Letters* 178, 151–164.
- Hebbeln, D., 2000. Flux of ice-rafted detritus from sea ice in the Fram Strait. *Deep-Sea Research II* 47, 1773–1790.
- Helland, P.E., Holmes, M.A., 1997. Surface textural analysis of quartz sand grains from ODP Site 918 off the southeast coast of Greenland suggests glaciation of southern Greenland at 11 Ma. *Palaeogeography, Palaeoclimatology, Palaeoecology* 135, 109–121.
- Helmke, J.P., Bauch, H.A., Röhl, U., Mazaud, A., 2005. Changes in sedimentation patterns of the Nordic seas region across the mid-Pleistocene. *Marine Geology* 215, 107–122.
- Henriot, J.P., Guidard, S., the ODP “Proposal 573” Team, 2002. Carbonate mounds as a possible example for microbial activity in geological processes. In: Wefer, G., Billet, D.S.M., Hebbeln, D., Jørgensen, B.B., Schlüter, M., van Weering, T.C.E. (Eds.), *Ocean Margin Systems*. Springer, Heidelberg, pp. 439–455.
- Higgs, R., 1979. Quartz-grain surface features of Mesozoic–Cenozoic sands from the Labrador and Western Greenland Continental Margins. *Journal of Sedimentary Petrology* 49, 599–610.
- Hill, P.R., Nadeau, O.C., 1984. Grain-surface textures of Late Wisconsinian sands from the Canadian Beaufort Shelf. *Journal of Sedimentary Petrology* 54, 1349–1357.
- Huvenne, V.A.I., Blondel, P., Henriot, J.P., 2002. Textural analyses of sidescan sonar imagery from two mound provinces in the Porcupine Seabight. *Marine Geology* 189, 323–341.
- Huvenne, V.A.I., Masson, D.D., Wheeler, A.J., 2009a. Sediment dynamics of a sandy contourite: the sedimentary context of the Darwin cold-water coral mounds, Northern Rockall Trough. *International Journal of Earth Sciences* 98, 865–884.
- Huvenne, V.A.I., Van Rooij, D., De Mol, B., Thierens, M., O'Donnell, R., Foubert, A., 2009b. Sediment dynamics and palaeo-environmental context at key stages in the Challenger cold-water coral mound formation: clues from sediment deposits at the mound base. *Deep-Sea Research I* 56, 2263–2280.
- Ingersoll, R.V., 1974. Surface textures of first cycle quartz sand grains. *Journal of Sedimentary Petrology* 44, 151–157.
- Jansen, E., Fronval, T., Rack, F., Channell, J.E.T., 2000. Pliocene–Pleistocene ice rafting history and cyclicity in the Nordic Seas during the last 3.5 Myr. *Paleoceanography* 15, 709–721.
- Kano, A., Ferdelman, T.G., Williams, T., Henriot, J.-P., Ishikawa, T., Kawagoe, N., Takashima, C., Kakizaki, Y., Abe, K., Sakai, S., Browning, E.L., Li, X., IODP Exp. 307 Scientists, 2007. Age constraints on the origin and growth history of a deep-water coral mound in the northeast Atlantic drilled during Integrated Ocean Drilling Program Expedition 307. *Geology* 35, 1051–1054.
- Kenyon, N., Belderson, R.H., Stride, A.H., 1978. Channels, canyons and slump folds between South-West Ireland and Spain. *Oceanologica Acta* 1, 369–380.
- Klages, M., Thiede, J., Foucher, J.-P., Crew, S.S., 2004. The Expedition ARKTIS XIX/3 of the Research Vessel POLARSTERN in 2003 – reports of Legs 3a, 3b and 3c. Reports on Polar and Marine Research. 488 pp.
- Knutz, P.C., Jones, E.J.W., Austin, W.E.N., van Weering, T.C.E., 2002. Glacimarine slope sedimentation, contourite drifts and bottom current pathways on the Barra Fan, UK North Atlantic margin. *Marine Geology* 188, 129–146.
- Konert, M., Vandenbergh, J., 1997. Comparison of laser grain size analysis with pipette and sieve analysis: a solution for the underestimation of the clay fraction. *Sedimentology* 44, 523–535.
- Laberg, J.S., Stoker, M.S., Dahlgren, K.I.T., de Haas, H., Hafliðason, H., Hjelstuen, B.O., Nielsen, T., Shannon, P.M., Vorren, T.O., van Weering, T.C.E., Ceramicola, S., 2005. Cenozoic alongslope processes and sedimentation in the NW European Atlantic margin. *Marine and Petroleum Geology* 22, 1069–1088.
- Lisiecki, L.E., Raymo, M.E., 2005. A Pliocene–Pleistocene stack of 57 globally distributed benthic  $\delta^{18}\text{O}$  records. *Paleoceanography* 20, PA1003. doi:10.1029/2004PA001071.
- Mahaney, W.C., 2002. Atlas of Sand Grain Surface Textures and Applications. Oxford University Press. 237 pp.
- Mahaney, W.C., Kalm, V., 1995. Scanning electron microscopy of Pleistocene tills in Estonia. *Boreas* 24, 13–29.
- Mahaney, W.C., Kalm, V., 2000. Comparative scanning electron microscopy study of oriented till blocks, glacial grains and Devonian sands in Estonia and Latvia. *Boreas* 29, 35–51.
- Mahaney, W.C., Stewart, A., Kalm, V., 2001. Quantification of SEM microtextures useful in sedimentary environmental discrimination. *Boreas* 30, 165–171.

- Manker, J.P., Ponder, R.D., 1978. Quartz grain surface features from fluvial environments of Northeastern Georgia. *Journal of Sedimentary Petrology* 48, 1227–1232.
- Maslin, M.A., Haug, G.H., Sarnthein, M., Tiedemann, R., 1996. The progressive intensification of northern hemisphere glaciation as seen from the North Pacific. *Geologische Rundschau* 85, 452–465.
- McCave, I.N., Hall, I.R., 2006. Size sorting in marine muds: processes, pitfalls, and prospects for paleoflow-speed proxies. *Geochemistry, Geophysics, Geosystems* 7, Q10N05. doi:10.1029/2006GC001284.
- McCave, I.N., Manighetti, B., Robinson, S.G., 1995. Sortable silt and fine sediment size/composition slicing: parameters for palaeocurrent speed and palaeoceanography. *Paleoceanography* 10, 593–610.
- McCave, I.N., Hall, I.R., Antia, A.N., Chou, L., Dehairs, F., Lampitt, R.S., Thomsen, L., van Weering, T.C.E., Wollast, R., 2001. Distribution, composition and flux of particulate material over the European margin at 47°–50°N. *Deep-Sea Research II* 48, 3107–3139.
- Michels, K.H., 2000. Inferring maximum geostrophic current velocities in the Norwegian–Greenland Sea from settling-velocity measurements of sediment surface samples: methods, applications, and results. *Journal of Sedimentary Research* 70, 1036–1050.
- Mienis, F., de Stigter, H.C., White, M., Duineveld, G., de Haas, H., van Weering, T.C.E., 2007. Hydrodynamic controls on cold-water coral growth and carbonate-mound development at the SW and SE Rockall Trough Margin, NE Atlantic Ocean. *Deep-Sea Research I* 54, 1655–1674.
- Mienis, F., de Stigter, H.C., de Haas, H., van Weering, T.C.E., 2009. Near-bed particle deposition and resuspension in a cold-water coral mound area at the Southwest Rockall Trough margin, NE Atlantic. *Deep-Sea Research I* 56, 1026–1038.
- Mudelsee, M., Statterger, K., 1997. Exploring the structure of the mid-Pleistocene revolution with advanced methods of time-series analysis. *Geologische Rundschau* 86, 499–511.
- New, A.L., Barnard, S., Herrmann, P., Molines, J.-M., 2001. On the origin and pathway of the saline inflow to the Nordic Seas: insights from models. *Progress in Oceanography* 48, 255–287.
- Øvrebo, L.K., Houghton, P.D.W., Shannon, P.M., 2006. A record of fluctuating bottom currents on the slopes west of the Porcupine Bank, offshore Ireland – implications for Late Quaternary climate forcing. *Marine Geology* 225, 279–309.
- Peck, V.L., Hall, I.R., Zahn, R., Grousset, F., Hemming, S.R., Scourse, J.D., 2007. The relationship of Heinrich events and their European precursors over the past 60 ka BP: a multi-proxy ice-rafted debris provenance study in the North East Atlantic. *Quaternary Science Reviews* 26, 862–875.
- Pingree, R., Le Cann, B., 1989. Celtic and Armorican slope and shelf residual currents. *Progress in Oceanography* 23, 303–338.
- Prins, M.A., Weltje, G.J., 1999. End-member modelling of siliciclastic grain-size distributions: the late Quaternary record of eolian and fluvial sediment supply to the Arabian Sea and its paleoclimate significance. In: Harbaugh, J. (Ed.), *Numerical Experiments in Stratigraphy: Recent Advances in Stratigraphic and Sedimentologic Computer Simulations: SEPM (Society for Sedimentary Geology) Special Publication*, pp. 91–111.
- Prins, M.A., Bouwer, L.M., Beets, C.J., Troelstra, S.R., Weltje, G.J., Kruk, R.W., Kuijpers, A., Vroon, P.Z., 2002. Ocean circulation and iceberg discharge in the glacial North Atlantic: inferences from mixing of sediment size distributions. *Geology* 30, 555–558.
- Reimer, P.J., Baillie, M.G.L., Bard, E., Bayliss, A., Beck, J.W., Bertrand, C.J.H., Blackwell, P.G., Buck, C.E., Burr, G.S., Cutler, K.B., Damon, P.E., Edwards, R.L., Fairbanks, R.G., Friedrich, M., Guilderson, T.P., Hogg, A.G., Hughen, K.A., Kromer, B., McCormac, G., Manning, S., Ramsey, C.B., Reimer, R.W., Remmele, S., Southon, J.R., Stuiver, M., Talamo, S., Taylor, F.W., van der Plicht, J., Weyhenmeyer, C.E., 2004. INTCAL04 terrestrial radiocarbon age calibration, 0–26 cal kyr BP. *Radiocarbon* 46, 1029–1058.
- Rice, A.L., Billet, D.S.M., Thurston, M.H., Lampitt, R.S., 1991. The Institute of Oceanographic Sciences Biological Programme in the Porcupine Seabight: background and general introduction. *Journal of the Marine Biological Association of the UK* 71, 281–310.
- Roberts, J.M., Wheeler, A.J., Freiwald, A., 2006. Reefs of the deep: the biology and geology of cold-water coral ecosystems. *Science* 312, 543–547.
- Roberts, J.M., Wheeler, A.J., Freiwald, A., Cairns, S., 2009. Cold-Water Corals. *The Biology and Geology of Deep-Sea Coral Habitats*. Cambridge University Press, 334 pp.
- Ruddiman, W.F., 1977. Late Quaternary deposition of ice-rafted sand in the subpolar North Atlantic (lat 40° to 65°N). *Geological Society of America Bulletin* 88, 1813–1827.
- Rüggeberg, A., Dullo, W.-C., Dorschel, B., Hebbeln, D., 2007. Environmental changes and growth history of a cold-water carbonate mound (Propeller Mound, Porcupine Seabight). *International Journal of Earth Sciences* 96, 57–72.
- Sakai, S., Kano, A., Abe, K., 2009. Origin, glacial–interglacial responses, and controlling factors of a cold-water coral mound in NE Atlantic. *Paleoceanography* 24, PA2213. doi:10.1029/2008PA001695.
- Setlow, L.W., 1977. Age determination of reddened coastal dunes in Northwest Florida, USA, by use of scanning electron microscopy. In: Whalley, W.B. (Ed.), *Scanning Electron Microscopy Study of Sediments, a Symposium (Symposium held at the Third Meeting of Geological Societies of the British Isles. University College of Wales, Swansea): Geo Abstracts LTD*, pp. 283–305.
- Shackleton, N.J., Backman, J., Zimmerman, H.B., Kent, D.V., Hall, M.A., Roberts, D.G., Schnitker, D., Baldauf, J.G., Despraires, A., Homrighausen, R., Huddleston, P., Keene, J.B., Kaltenback, A.J., Krumsick, K.O., Morton, A.C., Murray, J.W., Westberg-Smith, J., 1984. Oxygen isotope calibration of the onset of ice-rafting and history of glaciation in the North Atlantic region. *Nature* 307, 620–623.
- Shannon, P.M., McDonnell, A., Bailey, W.R., 2007. The evolution of the Porcupine and Rockall basins, offshore Ireland: the geological template for carbonate mound development. *International Journal of Earth Sciences* 96, 21–35.
- Sosdian, S., Rosenthal, Y., 2009. Deep-sea temperature and ice volume changes across the Pliocene–Pleistocene climate transitions. *Science* 325, 306–309.
- St. John, K., 2008. Cenozoic ice-rafting history of the central Arctic Ocean: terrigenous sands on the Lomonosov Ridge. *Paleoceanography* 23, PA1S05. doi:10.1029/2007PA001483.
- Stoker, M.S., Praeg, D., Hjelstuen, B.O., Laberg, J.S., Nielsen, T., Shannon, P.M., 2005. Neogene stratigraphy and the sedimentary and oceanographic development of the NW European Atlantic margin. *Marine and Petroleum Geology* 22, 977–1005.
- Stow, D.A.V., Faugères, J.-C., Howe, J.A., Pudsey, C.J., Viana, A.R., 2002. Bottom currents, contourites and deep-sea sediment drifts: current state-of-the-art. In: Stow, D.A.V., Pudsey, C.J., Howe, J.A., Faugères, J.-C., Viana, A.R. (Eds.), *Deep-Water Contourite Systems: Modern Drifts and Ancient Series, Seismic and Sedimentary Characteristics*. Geological Society, London, Memoirs, pp. 7–20.
- Strand, K., Passchier, S., Näsi, J., 2003. Implications of quartz grain microtextures for onset Eocene/Oligocene glaciation in Prydz Bay, ODP Site 1166, Antarctica. *Paleoceanography, Palaeoclimatology, Palaeoecology* 198, 101–111.
- Stuut, J.-B.W., Prins, M.A., Schneider, R.R., Weltje, G.J., Jansen, J.H.F., Postma, G., 2002. A 300-kyr record of aridity and wind strength in southwestern Africa: inferences from grain-size distributions of sediments on Walvis Ridge, SE Atlantic. *Marine Geology* 180, 221–233.
- Stuut, J.-B.W., Kasten, S., Lamy, F., Hebbeln, D., 2007. Sources and modes of terrigenous sediment input to the Chilean continental slope. *Quaternary International* 161, 67–76.
- Thomsen, L., Gust, G., 2000. Sediment erosion thresholds and characteristics of resuspended aggregates on the western European continental margin. *Deep-Sea Research I* 47, 1881–1897.
- Titschack, J., Thierens, M., Dorschel, B., Schulbert, C., Freiwald, A., Kano, A., Takashima, C., Kawagoe, N., Li, X., IODP Exp. 307 scientific party, 2009. Carbonate budget of a cold-water coral mound (Challenger Mound, IODP Exp. 307). *Marine Geology* 259, 36–46.
- Van Rooij, D., De Mol, B., Huvenne, V.A.I., Ivanov, M., Henriët, J.P., 2003. Seismic evidence of current-controlled sedimentation in the Belgica Mound province, upper Porcupine slope, southwest of Ireland. *Marine Geology* 195, 31–53.
- Van Rooij, D., Blamart, D., Richter, T., Wheeler, A., Kozachenko, M., Henriët, J.P., 2007. Quaternary sediment dynamics in the Belgica mound province, Porcupine Seabight: ice-rafting events and contour current processes. *International Journal of Earth Sciences* 96, 121–140.
- Van Rooij, D., Huvenne, V.A.I., Blamart, D., Henriët, J.-P., Wheeler, A.J., de Haas, H., 2009. The Enya mounds: a lost mound-drift competition. *International Journal of Earth Sciences* 98, 849–863.
- van Weering, T.C.E., De Stigter, H.C., Balzer, W., Epping, E.H.G., Graf, G., Hall, I.R., Helder, W., Khripounoff, A., Lohse, L., McCave, I.N., Thomsen, L., Vangriesheim, A., 2001. Benthic dynamics and carbon fluxes on the NW European continental margin. *Deep-Sea Research II* 48, 3191–3221.
- Wang, Y., Piper, D.J.W., Vilks, G., 1982. Surface texture of turbidite sand grains, Laurentian Fan and Sohm Abyssal Plain. *Sedimentology* 29, 727–736.
- Weaver, P.E., Wynn, R.B., Kenyon, N., Evans, J., 2000. Continental margin sedimentation, with special reference to the north-east Atlantic margin. *Sedimentology* 47, 239–256.
- Weltje, G.J., 1997. End-member modeling of compositional data: numerical–statistical algorithms for solving the explicit mixing problem. *Mathematical Geology* 29, 503–549.
- Weltje, G.J., Prins, M.A., 2003. Muddled or mixed? Inferring palaeoclimate from size distributions of deep-sea clastics. *Sedimentary Geology* 162, 39–62.
- Wheeler, A.J., Kenyon, N., Ivanov, M., Beyer, A., Cronin, B., McDonnell, A., Schenke, H.W., Akhmetzhanov, A.M., Satur, N., Zaragosi, S., 2003. Canyon heads and channel architecture of the Gollum Channel, Porcupine Seabight. In: Mienert, J., Weaver, P.E. (Eds.), *European Margin Sediment Dynamics: Side-scan Sonar and Seismic Images*. Springer, Heidelberg, pp. 183–186.
- Wheeler, A.J., Kozachenko, M., Beyer, A., Foubert, A., Huvenne, V.A.I., Klages, M., Masson, D.D., Olu-Le Roy, K., Thiede, J., 2005. Sedimentary processes and carbonate mounds in the Belgica mound province, Porcupine Seabight, NE Atlantic. In: Freiwald, A., Roberts, J.M. (Eds.), *Cold-water Corals and Ecosystems*. Springer-Verlag, Berlin, pp. 533–564.
- Wheeler, A.J., Beyer, A., Freiwald, A., de Haas, H., Huvenne, V.A.I., Kozachenko, M., Olu-Le Roy, K., Opperbecke, J., 2007. Morphology and environment of cold-water coral carbonate mounds on the NW European margin. *International Journal of Earth Sciences* 96, 37–56.
- White, M., 2007. Benthic dynamics at the carbonate mound regions of the Porcupine Sea Bight continental margin. *International Journal of Earth Sciences* 96, 1–9.
- White, M., Roberts, J.M., van Weering, T.C.E., 2007. Do bottom-intensified diurnal tidal currents shape the alignment of carbonate mounds in the NE Atlantic? *Geo-Marine Letters* 27, 391–397.
- Williams, T., Kano, A., Ferdelman, T.G., Henriët, J.-P., Abe, K., Andres, M.S., Bjerager, M., Browning, E.L., Cragg, B.A., De Mol, B., Dorschel, B., Foubert, A., Frank, T.D., Fuwa, Y., Gailloit, P., Gharib, J.J., Gregg, J.M., Huvenne, V.A.I., Léonide, P., Li, X., Mangelsdorf, K., Tanaka, A., Monteyes, X., Novosel, I., Sakai, S., Samarkina, V.A., Sasaki, K., Spiwack, A.J., Takashima, C., Titschack, J., 2006. Cold-Water Coral Mounds Revealed. *EOS (Transactions, American Geophysical Union)* 87, 525–526.